Synthesis and Characterization of Semi-IPN Hydrogels Composed of Sodium 2-Acrylamido-2-methylpropanesulfonate and Poly(ε-caprolactone) Diol for Controlled Drug Delivery

Amlika Rungrod[a], Apichaya Kapanya[a], Winita Punyodom[a,b], Robert Molloy[b,c], Anisa Mahomed[d] and Runglawan Somsunan[a,b*]

[a] Department of Chemistry, Faculty of Science, Chiang Mai University, Chiang Mai, 50200, Thailand
[b] Center of Excellence in Materials Science and Technology, Chiang Mai University, Chiang Mai, 50200, Thailand
[c] Materials Science Research Center, Faculty of Science, Chiang Mai University, Chiang Mai, 50200, Thailand
[d]Aston Institute of Materials Research, College of Engineering and Physical Sciences, Aston University, Birmingham, B4 7ET, United Kingdom

* E-mail: runglawan.s@cmu.ac.th

ABSTRACT

Semi-interpenetrating polymer network (semi-IPN) hydrogel of sodium 2-acrylamido-2-methylpropane sulfonate (Na-AMPS) and poly(ε-caprolactone) (PCL) diol for drug delivery applications was synthesized via free radical UV-photopolymerization technique using 2-hydroxy-4'-(2-hydroxyethoxy)-2-methylpropiophenone as an initiator and poly(ethylene glycol) diacrylate (PEGDA) as a crosslinker. The hydrogels' chemical structure and internal morphology have been explored using Fourier-transform infrared spectroscopy and scanning electron microscopy. The influence of PCL diol and PEGDA concentrations on the synthesized semi-IPN hydrogel properties was investigated. The semi-IPN hydrogel can increase the elasticity of the hydrogel while simultaneously providing enough water uptake and water retention. Furthermore, the semi-IPN hydrogel was non-cytotoxic to mouse fibroblasts L929 cells. Finally, ciprofloxacin (CIP) was used as a model drug and was efficiently encapsulated into the semi-IPN hydrogels. Drug loading capacity was enhanced with increasing PCL diol and CIP content. It was also observed that the PCL diol and CIP contents had a marked influence on the release profiles. Thus, the rate of release could be designed by changing the Na-AMPS to PCL diol ratio and CIP content. Drug release was found to be both diffusion and swelling-controlled in accordance with the Fickian and non-Fickian transport mechanisms. In the light of the results obtained, their easy formability, their appropriate mechanical and

physical properties make P(Na-AMPS)/PCL diol semi-IPN hydrogels are the potential candidates for use as drug carrier and controlled drug release materials in the biomedical field.

"*Keyworks: sodium 2-acrylamido-2-methylpropane sulfonate, poly(ε-caprolactone), semi-interpenetrating polymer network (semi-IPN) hydrogel, drug release*"

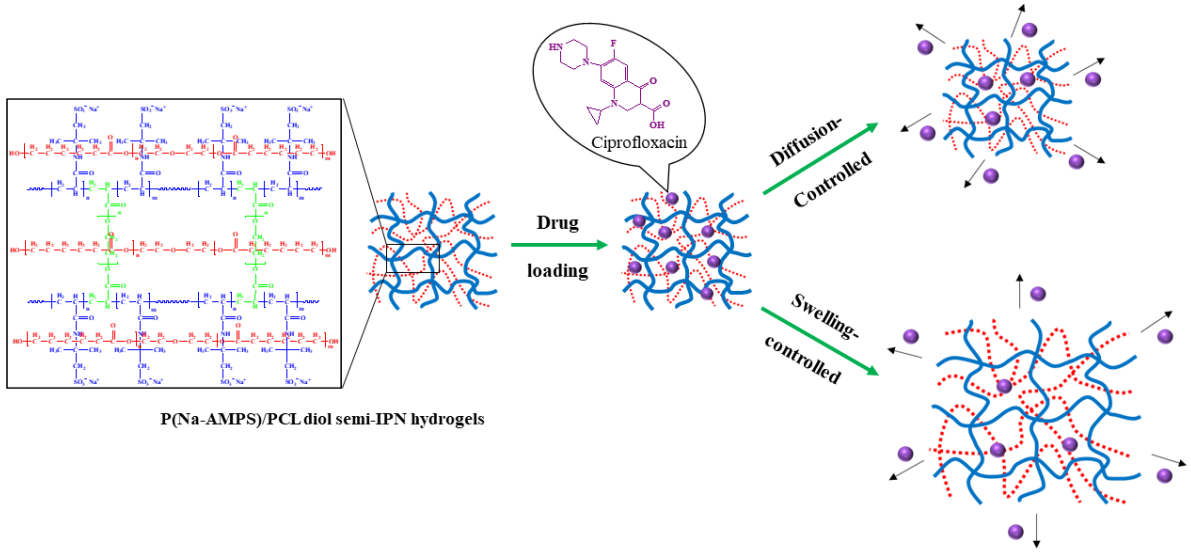

1. Introduction

Hydrogels are known as either physically or chemically crosslinked polymers with three-dimensional network structures that can keep water or biological fluids nearly 10 - 20 times greater than their original weight but do not dissolve [1]. This enables them to resemble soft tissues. They have been utilized in a wide range of biomedical applications, such as tissue engineering scaffolds, wound healing, subcutaneous cell delivery, drug delivery, sustained release of a bioactive agent, and so forth [2,3]. As drug delivery systems, hydrogels have been extensively studied for use in the biomedical and pharmaceutical area in recent years due to interesting properties of controlled release mechanisms, offering an advantage over common dosage forms. However, the low swelling ratio and fast release of loaded drugs from a conventional hydrogel often limits its application. Thus, the multi-polymer-based hydrogels synthesis is favored due to enhanced properties of tunability and effective drug release compared to a single component hydrogel [4].

Semi-interpenetrating (semi-IPN) polymerization is an efficient technique in which two polymers are blended and properties can be tuned by the feed compositions. Semi-IPN hydrogels are usually prepared by the “diffusion” of a linear polymer chain into a preformed

crosslinked polymer network. The two polymers are independent of each other but are physically interlinked. The linear polymer is physically bonded with crosslinked polymer network via electrostatic interactions, hydrogen bonding, Van der Waals forces, hydrophobic interactions or a combination of these [5]. The structures of semi-IPN hydrogels have interconnected porous network structures, which exhibit enhanced drug entrapment and controlled release profile compared to conventional hydrogels [6]. Furthermore, an interpenetration of linear polymers can lead to higher mechanical strength due to physical entanglements of linear polymers and the interactions between of the network and linear polymers [7,8]. Hydrophobic polymers can be combined with hydrophilic polymers by semi-IPNs to widen the range of the application of the hydrogel properties [9]. For example, the semi-IPN hydrogel fabrication by a combination of poly(ε-caprolactone), a hydrophobic polymer, with poly(acrylic acid), a hydrophilic polymer, for use as artificial cartilages [10] and controlled drug delivery [11].

Sodium 2-acrylamide-2-methylpropanesulfonate (Na-AMPS) is a hydrophilic ionic monomer extensively used in the synthesis of hydrogels. Na-AMPS has strongly ionizable sulfonic ($-SO_3H$) groups which have the ability to dissociate over the entire pH range and thus part pH-independent swelling characteristic [6]. However, the tensile strength of P(Na-AMPS) hydrogels is not high enough for some applications, and it has low strength and toughness due to the lack of an effective energy dissipation mechanism [12]. To overcome this weak point, P(Na-AMPS) could be combined with a polymer that has higher mechanical properties. In this work, poly(ε-caprolactone) (PCL) was chosen to form a blend with P(Na-AMPS) hydrogel. PCL is a hydrophobic polymer prepared by ring-opening polymerization of the ε-caprolactone monomer. This monomer contains one relatively polar ester and five non-polar methylene groups, enabling PCL to have high-molecular-chain flexibility and great utilization. The US Food and Drug Administration (FDA) describes PCL as a biodegradable polymer that exhibits non-toxic behavior and has shown to be biocompatible in several medical applications. Thus, PCL has been used in applications such as artificial permeation of membranes, food packaging, and applications related to the biomedical field [13].

Among the antibiotics drugs, ciprofloxacin (CIP) is one of the most widely used. It is effectively used to treat various diseases like osteomyelitis, diverticulitis, gonococcal infections, respiratory infections, urinary treat infections, and a variety of gram-negative and gram-positive bacterial infections. CIP belongs to the class of systemic fluoroquinolones and is thus a sparingly water-soluble drug [14,15]. Currently, there is a need to improve the

pharmacodynamics and pharmacokinetic profiles of the controlled drug-release systems. In order to improve bioavailability, many researchers have investigated various carriers for sustained CIP delivery. Basu, S. et al. designed green synthesis of Ag-nanocomposite semi-IPN hydrogels to deliver CIP antibiotic drugs and then also studied the swelling behavior. Its percentage release of CIP was 95% after 350 min [16]. Kajjari, P. B. et al. synthesized an acrylamide-graft-guar gum blend with a chitosan interpenetrating polymer network hydrogel for delivery of CIP. This released approximately 60% within 12 h [17]. Alshhab, A. et al. prepared polyelectrolyte multilayer films from sodium alginate and poly(4-vinylpyridine) for CIP release. They found that the percentage of drug release was 65% within 24 h [18]. Similarly, García,M. C. et al. prepared a hydrogel composed of an ionic complex from a dendronized polymer for CIP delivery that released 47% within 24 h [19].

Based on the above, the aim of this study is to understand the effect of hydrogel structure and morphological properties on controlled release of antibiotic drugs. Therefore, the semi-IPN hydrogel was designed in such a way as to improve the mechanical properties, drug entrapment and control drug release profiles. Na-AMPS and PCL diol were combined to produce a semi-IPN hydrogel for sustained delivery of CIP. Nevertheless, the combination of hydrophilic Na-AMPS with a hydrophobic polymer, in this case PCL diol, is very challenging. The semi-IPN hydrogels were fabricated by free radical UV-photopolymerization crosslinked with poly(ethylene glycol) diacrylate (PEGDA). The effect of PCL diol and PEGDA crosslinker concentrations on parameters such as crosslinking density, water uptake, water retention and mechanical properties were studied in detail. The capacity of water uptake and water retention were measured as a time function. The mechanical properties were examined by tensile test. Cytocompatibility was determined under *in vitro* conditions with mouse fibroblasts L929 cells. In addition, CIP was incorporated into the hydrogel to study its controlled release. In this research, the drug release in a medium at 37 ℃ and pH 7.4, which mimics the normal physiological environment, was studied. The effect of Na-AMPS/PCL diol ratios shed light on their release profile. Hydrolytic degradation analysis was also undertaken to confirm the stability of the hydrogel as well as the drug release mechanism. This research therefore describes the development of a new type of hydrogel as a controlled drug delivery system for use in the biomedical field, such as in antibacterial wound dressings.

2. Experimental

2.1. Materials

Poly(ε-caprolactone) diol (PCL diol, $\bar{M}_n$ ~530), 2-acrylamido-2-methylpropane sulfonic acid (AMPS) monomer, poly(ethylene glycol) diacrylate (PEGDA, $\bar{M}_n$ ~575) and 2-hydroxy-4′-(2-hydroxyethoxy)-2-methylpropiophenone (Irgacure 2959) were all purchased from Sigma-Aldrich and used as received without further purification. HPLC grade dimethyl sulfoxide (DMSO), a solvent for hydrogel synthesis, was purchased from Sigma-Aldrich. Ciprofloxacin antibiotic model drug was purchased from Sigma Aldrich. The water employed in all experiments was distilled water.

2.2 Preparation of P(Na-AMPS)/PCL diol semi-IPN hydrogels

Na-AMPS was prepared by neutralizing the AMPS monomer with sodium hydroxide in an aqueous solution to pH 7.4. The Na-AMPS solution was then dried at 40.0 ± 1.0 ℃ for 5 days until Na-AMPS powder was obtained for further polymerization. The P(Na-AMPS)/PCL diol semi-IPN hydrogel was prepared by dissolving prepared Na-AMPS powder (50 %w/v) with PCL diol at different concentrations (0, 10, 30, and 50 %wt of Na-AMPS) in DMSO 10 ml. The mixture was stirred with a mechanical stirrer at room temperature for 3 h to produce a homogeneous mix. The PEGDA concentrations ranging from 0.50 to 2.00 %wt of Na-AMPS was then added as a crosslinking agent. Irgacure 2959 photoinitiator at 0.10 %wt of Na-AMPS was then added to the solution and stirred vigorously at room temperature for 1 h to completely dissolve. Subsequently, the mixture solution was transferred into a mold. The mold comprised of two glass plates covered by a Teflon® sheet on one side, with thickness controlled by a spacer. The prepared mold which contained the mixture solution was placed in an aluminium cabinet with a commercially available UV lamp (Philips Solarium Model MD 1-15 UV lamp). The lamp comprised four parallel Cleo 15 W fluorescent tubes that emitted UV light in the 315 - 400 nm wavelength range [20]. The hydrogel was synthesized at room temperature for 15 min. Once polymerization was complete, the hydrogel samples were carefully removed from the mold and kept in a plastic bag before further characterization. For purification, the prepared hydrogels were cut into the square piece (1.0 × 1.0 cm^2) and then washed with an excess of distilled water for 3 days. The water was refreshed twice daily to remove residual unreacted monomers and other impurities. Finally, the hydrogels were dried at a temperature of 45.0 ± 1.0 ℃ for 3 days to constant weight and stored in a desiccator for further use.

2.3 Fourier transform infrared spectroscopy (FTIR)

Hydrogel samples were analyzed using a Fourier transform infrared spectroscope (Bruker-Tensor 27, German) in the region of 4000 to 400 cm^{-1}. The hydrogel samples were prepared with a KBr pellet technique. Before the analysis, they were dried under vacuum oven until a reached constant weight. The hydrogels were then ground and mixed with KBr powder and pressed into pellets under pressure, while PCL diol was measured by the NaCl discs method. OPUS 7.2 analytical software was used in conjunction with the FTIR to process the data.

2.4 Swelling properties measurements

Pre-weighed dry hydrogels were immersed directly in distilled water and kept in an incubator at a temperature of 35.0 ± 1.0 ℃. The swollen hydrogels were taken out and weighed after wiping off the surface water with absorbent paper at the determined time intervals. Each sample were continually measured until reaching a constant weight. The water uptake (*WU*) was determined according to the following equation:

$$WU\,(\%) = \frac{W_t - W_d}{W_d} \times 100 \qquad (1)$$

where W_t is the weight of the swollen hydrogel at time t, and W_d is the weight of the dried hydrogel. Averaging from three measurements of all results are obtained.

2.5 Water retention measurements

Dried hydrogel samples were immersed in distilled water at room temperature until an equilibrium was reached. The swollen hydrogel samples were then swiftly transferred into an incubator at a temperature of 35.0 ± 1.0 ℃ and 55 - 60 % of relative humidity. The hydrogels weight changes were recorded during the water evaporation of hydrated hydrogels at various time intervals. Water retention (*WR*) in the hydrogel was defined as:

$$WR\,(\%) = \frac{W_t - W_d}{W_{eq} - W_d} \times 100 \qquad (2)$$

where W_t is the weight of hydrogel at time t during the shrinking process, W_{eq} is the weight of the equilibrium swollen hydrogel and W_d is the weight of the dried hydrogel. The analyses were carried out in triplicates to obtain averaged values.

2.6 Mechanical properties by tensile testing

Tensile testing of hydrogel samples was performed on a universal mechanical testing machine (LRX, LLOYD) with a preload of 0.01 N at room temperature. The synthesized hydrogels (after polymerization) were kept in a plastic bag and allowed to reach equilibrium at room temperature for 24 h before tensile testing. Rectangular hydrogel samples (10×70 mm^2) were tested at a constant speed rate of 10 mm/min. The hydrogel specimen was fixed between the two clamps and a tensile force applied in order to vertically stretch the hydrogel to a gauge length of 50 mm. The stress-strain curves were recorded, and the tensile modulus obtained from the linear slope. Five samples per measurement were performed and the obtained values were averaged.

2.7 Scanning electron microscopy (SEM)

SEM micrographs of the hydrogels were observed on a JSM-IT300. The hydrogels were swollen in distilled water to equilibrium (for at least 24 h) and then freeze-dried. The freeze-dried hydrogels were coated with gold. The photographed microstructural of the hydrogels was observed by SEM which is operated at an acceleration of 15 kV and ×100 magnification.

2.8 Crosslink density

Flory-Rehner theory was used for calculating crosslink density (*XD*) of hydrogels using the following equation:

$$XD = \frac{M_c}{M_r} \tag{3}$$

where M_r is molar masses of the repeat units that make up the hydrogel and is calculated from the following equation:

$$M_r = \frac{m_{Na\text{-}AMPS} M_{Na\text{-}AMPS} + m_{PCL\ diol} M_{PCL\ diol} + m_{PEGDA} M_{PEGDA}}{m_{Na\text{-}AMPS} + m_{PCL\ diol} + m_{PEGDA}} \tag{4}$$

where $m_{Na\text{-}AMPS}$, $m_{PCL\ diol}$ and m_{PEGDA} are the masses of the monomer (Na-AMPS), polymer (PCL diol), and crosslinker (PEGDA), while $M_{Na\text{-}AMPS}$, $M_{PCL\ diol,}$ and M_{PEGDA} are the molar masses of Na-AMPS, PCL diol and PEGDA, respectively.

According to Flory-Rehner theory, M_c is the average molecular weight between crosslinks, representing the degree of crosslinking of the hydrogel network between two

adjacent crosslinks. The average molecular weight between adjacent crosslinks was calculated using:

$$M_c = \frac{d_p V_s \left(V_{2,s}^{1/3} - \frac{V_{2,s}}{2}\right)}{ln(1 - V_{2,s}) + V_{2,s} + \chi V_{2,s}^2} \quad (5)$$

where V_s is the molar volume of solvent (water = 18.0 ml/mol) and $V_{2,s}$ is the volume fraction of swollen hydrogel in an equilibrium state. The $V_{2,s}$ indicates the capacity of hydrogel to allow the diffusion of the solvent into the network structure, which can be calculated by using:

$$V_{2,s} = 1/\left[1 + \frac{d_p}{d_s}\left(\frac{m_s}{m_d} - 1\right)\right] \quad (6)$$

where d_p and d_s are densities (g/ml) of the hydrogel and solvent (water = 0.99904 g/cm^3 at 35.0 ± 1.0 °C), respectively. m_s and m_d are the masses (g) of the swollen and dried hydrogel, respectively. While χ indicates the Flory-Huggins polymer (hydrogel)-solvent interaction parameter.

To investigate the compatibility between the monomer and polymer in the hydrogels, the solvent interaction parameter (χ) was measured according to Flory-Huggins theory as follows:

$$\chi = \frac{\ln(1 - V_{2,s}) + V_{2,s}}{V_{2,s}^2} \quad (7)$$

The d_p of each hydrogel was determined from:

$$d_p = \frac{m}{V} = m/\left(\frac{W \times L}{H}\right) \quad (8)$$

where W, L and H are width, length and height (cm) of the swollen hydrogel in an equilibrium state, respectively. m is the mass (g) of the dried hydrogel.

Thus, to calculate the XD of the hydrogels, the values of m_s and d_p are obtained by measuring the swollen hydrogel. This enables $V_{2,s}$ of each semi-IPN hydrogel to be obtained first. Then consequently χ and M_c can be calculated.

2.9 Evaluation of cytotoxicity

The cytotoxicity assay of the hydrogels produced was performed by the MTT colorimetric technique based on the ISO 10993-5 standard test method. Before the assay, the

hydrogels were sterilized by autoclaving at 121 °C for 15 min. The sterilized hydrogels (0.25 cm^2) were immersed in 1.2 ml MEM at 37.0 ± 1.0 ℃ for 24 ± 2 h prior to acquiring an extract. At the same time, 1 × 10^5 cell/ml mouse fibroblasts L929 cells were suspended in MEM complete medium and seeded into a 96-well plate. The 96-well culture plate was incubated for 24 ± 2 h at 37.0 ± 1.0 ℃, 5 ± 0.1 % CO_2 and 95 ± 5 % relative humidity to obtain a confluent monolayer of cells prior to testing. The MEM medium was completely removed from the wells, replaced with the extract obtained from the hydrogel and incubated for another 24 ± 2 h. After incubation, MTT solution was added to each well, and the cells were incubated at 37.0 ± 1.0 ℃ for a further 2 h. MTT was then removed and DMSO added to each well to dissolve the MTT formazan purple crystals. The optical density of the formazan solution was determined by a Microplate reader at 570 nm. A 'Thermanox' (Nunc) coverslip with the surface area to volume extraction ratio of 6 cm^2/ml was used as a negative control.

2.10 Drug loading and entrapment efficiency

Ciprofloxacin (CIP) was chosen as the drug model and loaded into the semi-IPN hydrogels by the swelling-diffusion technique. Dried hydrogels were placed in an aqueous solution of the drug with various CIP concentrations ranging from 0.05 to 0.25 mg/ml followed by refrigerated (~ 4 ℃) for 24 h. After 24 h, the remaining drug solution was decanted off and analyzed using a UV spectrophotometer (Drawell) at 275 nm to determine the amount of unloaded CIP. This value was used to determine the CIP entrapment efficiency of hydrogels. The swollen hydrogels were dried at 40 ℃ for 24 h to obtain drug-loaded hydrogels and used for experiments of release. The drug loading (DL) and entrapment efficiency (EE) of the hydrogels were calculated using the following equations:

DL (%) = weight of the drug in hydrogel / weight of hydrogel × 100 (9)

EE (%) = content of drug in hydrogel / theoretical content of drug × 100 (10)

2.11 In vitro controlled drug release study

The *in vitro* drug-release was completed using experimental conditions mimicking the tissue medium, such as pH 7.4 phosphate buffer (PBS) at 37.0 ± 1.0 ℃. The experimental procedure involved the dried drug-loaded hydrogels being dipped into vials containing 5 ml of PBS solution. At specific time intervals, the solution was completely removed. In order to maintain the release medium volume, the same time, an equal volume (5 ml) of PBS solution replenished the solution that was completely removed. The amount of CIP released was

calculated using previously determined calibration curves. The cumulative percent of drug released from the hydrogels was plotted against time. Each measurement was performed in triplicate and averaged. In order to evaluate the mechanism of CIP release from the hydrogels, the data were fitted on a series of equations of mathematical models, such as Zero-order, First-order, Higuchi, Korsmeyer-Peppas and Hixson-Crowell. The kinetic models were expressed as the following equation:

$$\text{Zero-order model : } \frac{Q_t}{Q_o} = k_o \, t \tag{11}$$

$$\text{First-order model : } \log \frac{Q_t}{Q_o} = \log Q_o - \frac{k_1 \, t}{2.303} \tag{12}$$

$$\text{Higuchi order : } Q = k_H \, t^{1/2} \tag{13}$$

$$\text{Korsmeyer-Peppas model : } \log \frac{Q_t}{Q_o} = \log k_{KP} + n \log t \tag{14}$$

$$\text{Hixson-Crowell : } Q_o^{1/3} - Q_1^{1/3} = k_{HC} \, t \tag{15}$$

where Q_t represents the amount of drug release at time t, Q_o is the initial drug amount, k is the rate constant, and n is the release exponent indicative the drug transport mechanism.

2.12 In vitro hydrolysis degradation analysis

The weight of dried hydrogels was recorded, immersed in 5 ml of PBS solution (pH 7.4) and placed in an incubator at a temperature of 37.0 ± 1.0 ℃. At selected time points, the hydrogels were taken out, dried and weighed again for weight loss analysis. The medium was changed and replenished with fresh medium every week. The degradation of each hydrogel was calculated using the following equation:

$$\text{Degradation (\%)} = ((\text{Initial weight-Weight after degradation})/\text{Initial weight}) \times 100 \tag{16}$$

2.13 Statistical analysis

Figures were generated with software of Graph Pad Prism version 6.00 used for statistical analysis. Primary statistical analysis of data was performed by one-way analysis of variance (ANOVA) with Tukey's post hoc method to multiple comparisons and the differences determined in every tested group. All the analyses were carried out in three or five repetitions to find mean and standard deviation values. The statistical significance was considered at $p < 0.05$.

3. Results and discussion

3.1 Probable mechanism and physical properties of P(Na-AMPS)/PCL diol semi-IPN hydrogel formation

In this study, various compositions of semi-interpenetrating polymer network (semi-IPN) hydrogels were synthesized from Na-AMPS and PCL diol, using various concentrations of poly(ethylene glycol) diacrylate (PEGDA) as a crosslinker and 1-[4-(2-hydroxyethoxy)-phenyl]-2-hydroxy-2-methyl-1-propanone (Irgacure 2959) as a photoinitiator. Semi-IPN hydrogels were synthesized by the photoinitiation method using UV light. This method was found to be the most accessible and productive for controlling the polymerization reactions in a short period. In addition, Irgacure 2959 is one of the most widely used photoinitiators for hydrogel synthesis through the free-radical species created during UV irradiation due to its high availability and easily controlled the physical and mechanical properties of the hydrogel [21].

The polymerization mechanism of semi-IPN hydrogels composed of Na-AMPS and PCL diol is described in Fig.1. First, the Irgacure 2959 molecule is cleaved to produce free-radical molecules by UV decomposition. These photoinitiator radicals are then attracted to a Na-AMPS monomer molecule, which opens its double bond and produces a new radical center on the Na-AMPS monomer molecule resulting in the point of polymerization. The propagation stage then follows, with the latter continuously adding on more Na-AMPS monomer and growing into a chain. As the chain propagation reactions proceed, the polymer chains are reacted with the end vinyl groups of PEGDA to form a crosslinked structure. During this process, linear PCL diol chains can also interpenetrate into the network. The formation process of semi-IPN hydrogel and its structure can be inferred according to the FTIR and SEM analysis results, as explained below.

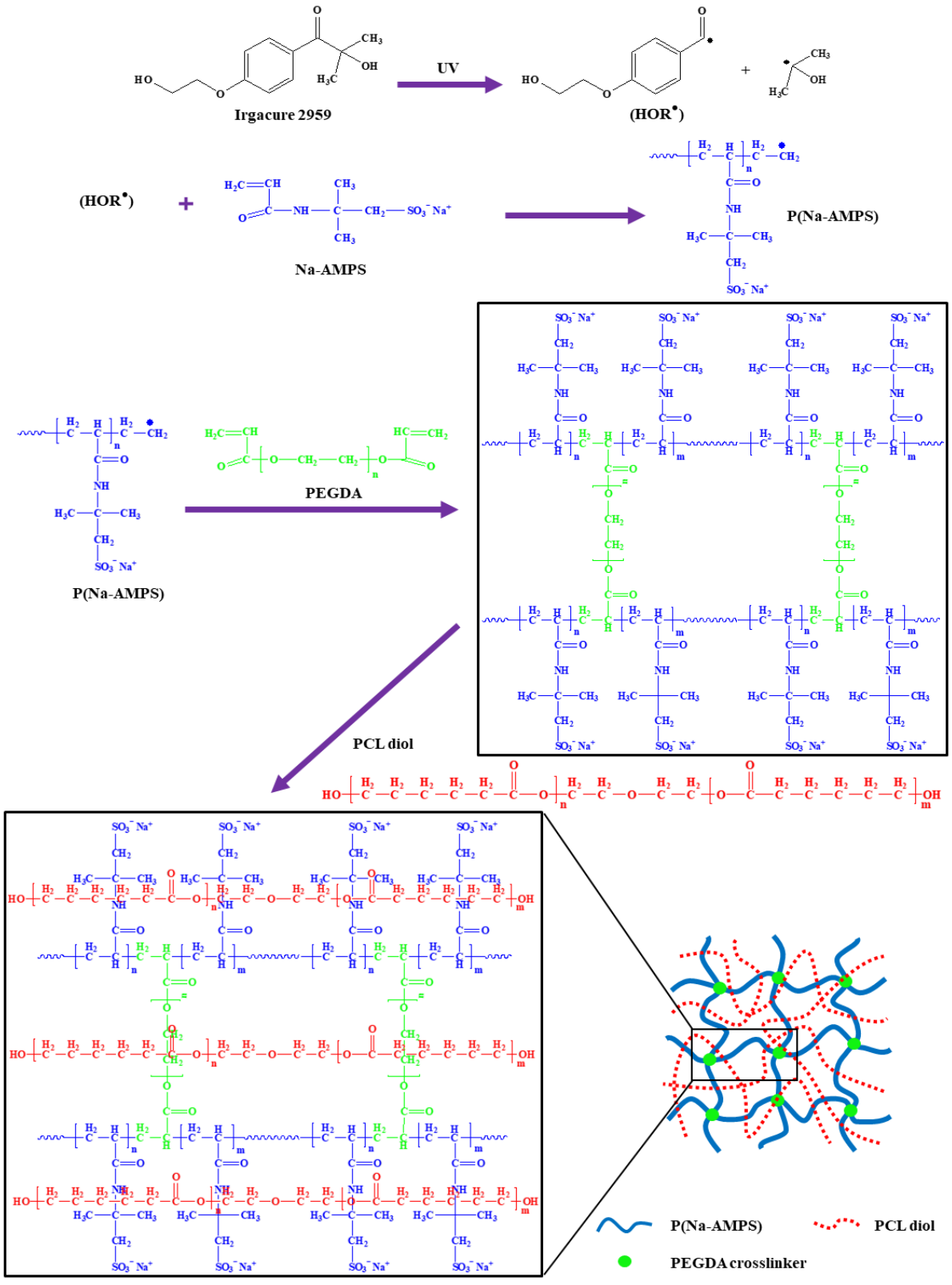

Fig.1. Proposed mechanistic pathway for preparation of P(Na-AMPS)/PCL diol semi-IPN hydrogels.

The physical properties of the hydrogels polymerized with different compositions of Na-AMPS and PCL diol at constant PEGDA 0.75 %w/$w_{Na\text{-}AMPS}$ are shown in Fig. 2. It can be seen that these differ according to the formulation. The physical appearance of the hydrogel without PCL diol was transparent, but the hydrogel formulations containing PCL diol became increasingly turbid with PCL diol concentration. This was occurred from phase separation between the P(Na-AMPS) network matrix and the dispersed PCL diol domains. However, the hydrogels with PCL diol also demonstrated that the properties of physical and mechanical were improved (tear strength), with flexibility also increasing with PCL diol.

Moreover, the PEGDA crosslinker concentration also influenced the physical properties of the hydrogel. The tensile test results (Section 3.5) indicated that increasing the crosslinker concentration resulted in brittle hydrogels with low tear strength.

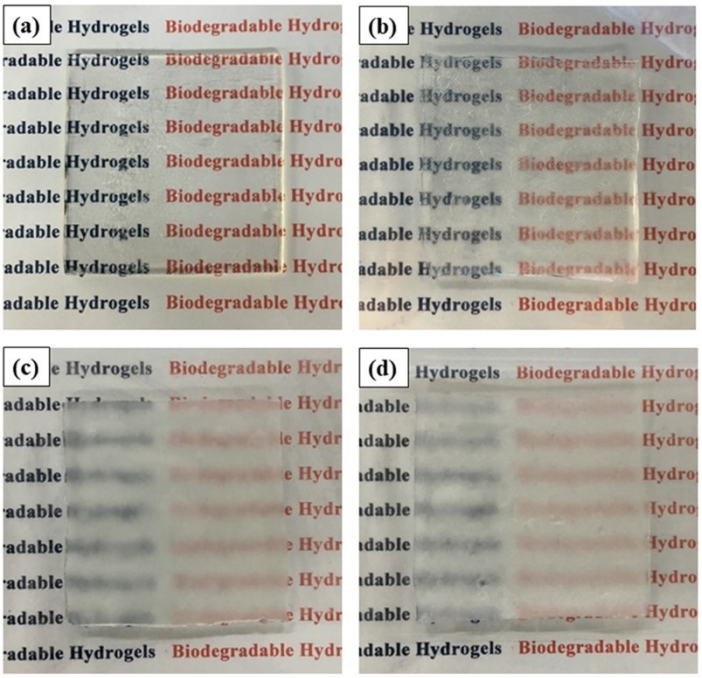

Fig. 2. Comparison of the physical appearances of hydrogels at constant PEGDA 0.75 %w/$w_{Na\text{-}AMPS}$ with varying PCL diol concentration of (a) 0, (b)10, (c) 30 and (d) 50 %w/$w_{Na\text{-}AMPS}$.

3.2 FTIR spectral analysis

FTIR spectroscopy was used to confirm the synthesized semi-IPN hydrogel structure with different compositions of Na-AMPS and PCL diol at constant PEGDA 0.75 %w/$w_{Na\text{-}AMPS}$. The FTIR spectrum of P(Na-AMPS)/PCL diol semi-IPN is reported in Fig. 3 and compared with those of PCL diol and a pure P(Na-AMPS) hydrogel. For PCL diol, the absorption bands at 2943 cm^{-1} correspond to C-H vibrations of the -CH_2 group, the peak at 1732 cm^{-1} corresponds to C=O vibrations and the absorption bands at 1167 cm^{-1} corresponds to the C-O-C vibrations. The absorption broads relating to the terminated hydroxyl groups (-OH) appear at 3080 - 3700 cm^{-1} [10]. For single P(Na-AMPS) hydrogel, the spectrum was characterized with absorption bands at 1047 cm^{-1} and 1190 cm^{-1} correspond to symmetric and asymmetric stretching of S=O respectively. The absorption bands represented at 2980 cm^{-1} was assigned to C-H stretching of CH_2 groups, and absorption bands at 1655 cm^{-1} and 1559 cm^{-1} were assigned to C=O stretching of amide-I and N-H bending of amide-II, respectively [6]. Analysis of P(Na-AMPS)/PCL diol semi-IPN hydrogel, indicated the appearance of new absorption bands with the characteristic peaks for both PCL diol and Na-AMPS present with a bit of position shifting. Compared to the IR spectrum of single P(Na-AMPS) hydrogel, a semi-IPN hydrogel with PCL diol at 50 %w/$w_{Na\text{-}AMPS}$ showed new absorption bands at approximately 1169 cm^{-1} and 1732 cm^{-1} correspond to the C-O-C and C=O vibration of PCL diol, respectively. In addition, the C-O-C and C=O characteristic stretching of PCL diol strengthened with increasing PCL diol content in semi-IPN hydrogels. These further confirmed the presence of PCL diol within semi-IPN hydrogel structures after purification. The intensity ratio of 1732 cm^{-1} (C=O of PCL diol) to 1047 cm^{-1} (S=O of Na-AMPS) is plotted in Fig. 4. With increasing PCL diol content, the intensity ratio gradually increases. From the FTIR results, it can be concluded that PCL diol was incorporated within the hydrogel structure and the structure of semi-IPN was formed, similar to that already presented in the case of other semi-IPN hydrogels [22,23].

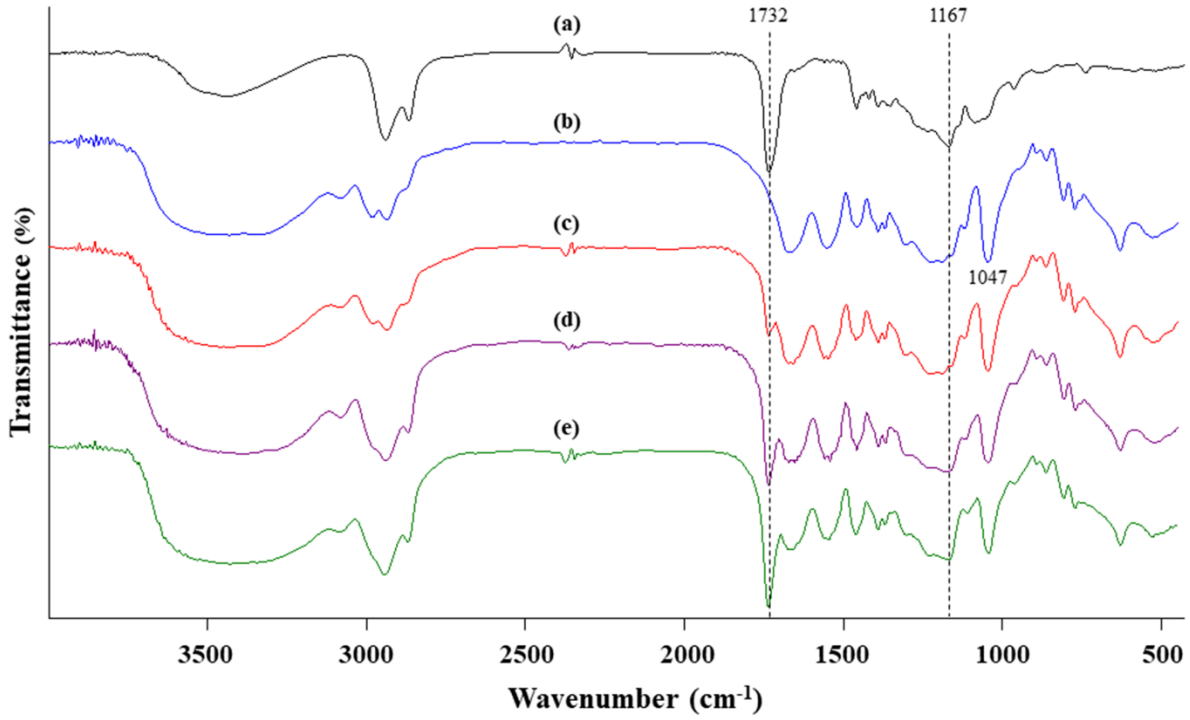

Fig. 3. The FTIR spectra of PCL diol (a), and hydrogels containing PEGDA 0.75 %w/$w_{Na\text{-}AMPS}$ and varying PCL diol concentrations of 0 (b), 10 (c), 30 (d) and 50 %w/$w_{Na\text{-}AMPS}$ (e).

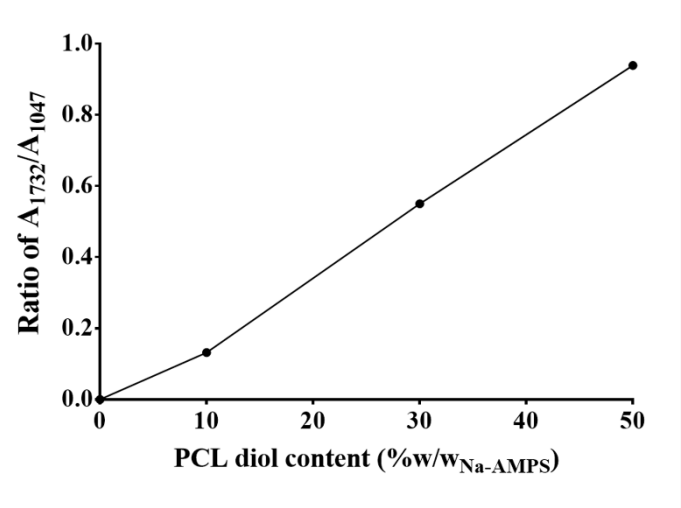

Fig. 4. The intensity ratio of 1732 cm^{-1} to 1047 cm^{-1} of hydrogel at constant PEGDA 0.75 %w/$w_{Na\text{-}AMPS}$ with different PCL diol contents.

3.3 Swelling properties test

Commonly, swelling properties under *in vitro* tests play an important role for the prospective evaluation of biomaterials. Highly water-swollen hydrogels are considered promising materials for controlled drug release. The swelling behavior of hydrogels depends on the composition of hydrogels, the crosslinking density, the overall hydrophilicity of material, the characteristics of the external solution, such as the environment temperature, the ionic strength and pH of the aqueous media [24]. The dynamics of the water sorption process were studied gravimetrically. All hydrogels were immersed in water at 35.0 ± 1.0 ℃, and their water uptake was measured overtime at different time intervals. The water uptake was calculated and the water uptake-time profile of the semi-IPN hydrogel for each composition of Na-AMPS and PCL diol (PCL diol 0 - 50 %wt of Na-AMPS), with various concentrations of PEGDA crosslinker (0.50 - 2.00 %wt of Na-AMPS), are shown in Fig. 5. The water uptake of all semi-IPN hydrogels increased sharply during the initial period (t < 60 min) and then plateaued.

Fig. 6(a) shows the influence of the crosslinker and PCL diol concentration on the water uptake at equilibrium (*EWU*) of semi-IPN hydrogels. The equilibrium swelling data showed that the *EWU* values of hydrogel are very high, these were found to be between 5,400 to 35,800 %. It was found that the *WU* for hydrogels decreased with increasing the PEGDA crosslinker content due to an increase in crosslinking density and thus a tighter three-dimensional network. This leads to limited extensibility of the network chain preventing the ingress of water molecules into the hydrogel network leading to a reduced water uptake of the hydrogels. It is a known fact that the water uptake can be decreased by increasing the amount of crosslinking density [25–27]. In the case of PCL diol, the incorporation of PCL diol at 10 %w/$w_{Na\text{-}AMPS}$ appeared to increase the water uptake of the semi-IPN compared to the pure P(Na-AMPS) hydrogel (PCL diol at 0 %w/$w_{Na\text{-}AMPS}$). A possible explanation is that an increase in the PCL diol content helps bring about a higher water uptake and a looser network. This causes free volume resulting in easier diffusion of the water molecules into the hydrogel network. Similar results can also be observed for the semi-IPN hydrogel based on Salecan and poly(N,N-dimethylacrylamide-co-2-hydroxyethylmethacrylate) hydrogel system [8]. Increasing the PCL diol content above 10 %w/$w_{Na\text{-}AMPS}$, the hydrogel network becomes more hydrophobic and consequently absorbs lower water. It is known that the hydrophobic groups (-CH_2CH_2) in the PCL diol structure, correspond to polymer-polymer hydrophobic interactions, resulting in a remarkable reduction in water adsorption [28]. The second possible reason that the water

uptake of the hydrogel decreased with incorporation of PCL diol above 10 %w/$w_{Na\text{-}AMPS}$ is related to network structure. Higher amounts of PCL diol lead to the formation of a very high number of polymer chains that penetrate the network structure, reduce free volume between network chains therefore limiting the ingress of water molecules into the network which results in lower water adsorption.

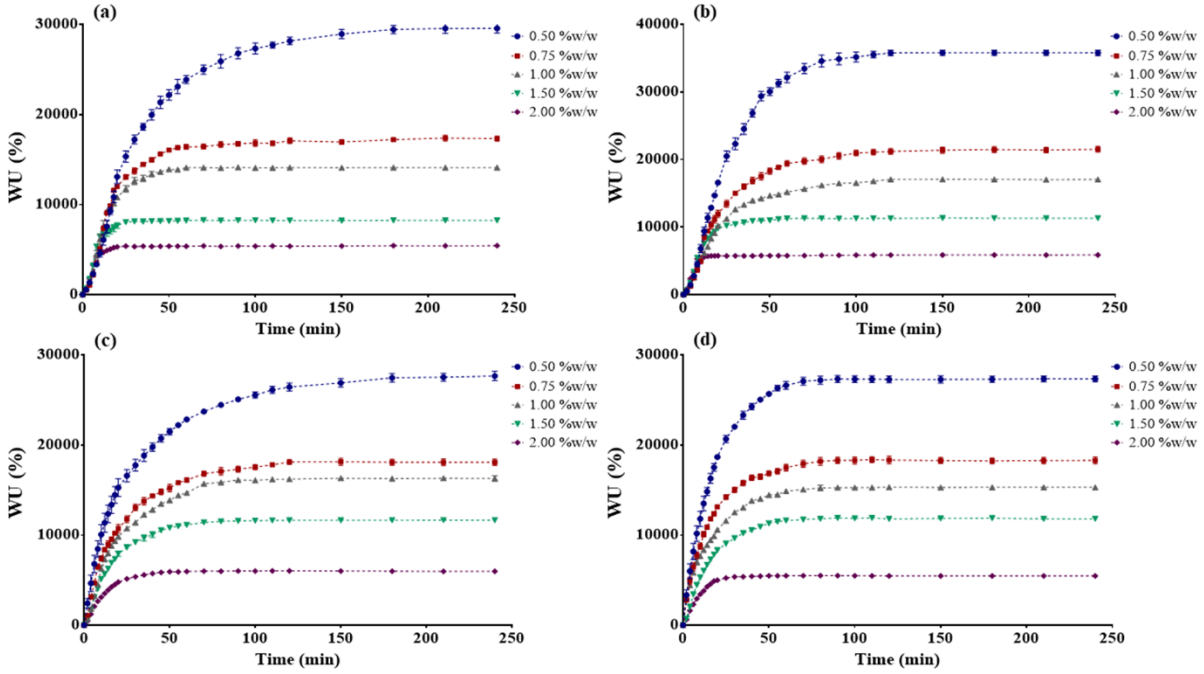

Fig. 5. The water uptake-time profile of hydrogel in different concentration of PEGDA crosslinker (0.50 - 2.00 %w/$w_{Na\text{-}AMPS}$) with various concentrations of PCL diol at (a) 0, (b)10, (c) 30 and (d) 50 %w/$w_{Na\text{-}AMPS}$.

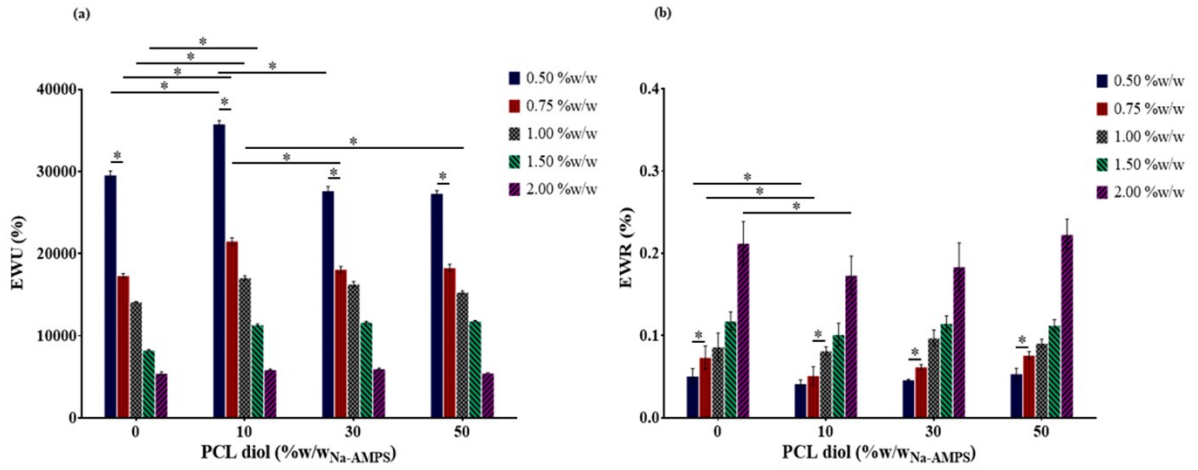

Fig. 6. The water uptake (a) and water retention (b) at equilibrium of the hydrogels in different compositions of Na-AMPS and PCL diol at various concentrations of PEGDA crosslinker (* $p < 0.05$).

3.4 Water retention test

The crucial factors affecting water retention are the crosslink density (ratio of monomer to crosslinker) and the hydrophilic group associated to the hydrogel backbone. Thus, the effects of the Na-AMPS and PCL diol composition with various PEGDA crosslinker concentrations was studied in terms of their influence on water retention of the hydrogel.

The water within the hydrogel can be described as a spectrum of non-freezing water (or non-freezing-bound water), freezing-bound water (or intermediate water), and free water (or freezing water). When the water shell that is on contact to the ions on the polymer backbone, non-freezing water occurs in the first layer. It is tightly interaction to the surface of polymer. Then, the next layers will deposit in the following by the water molecules moderately interacted with the polymer surface, called the intermediate water. This water type involves water-surface and water-water interaction. The non-freezing and intermediate waters are influenced by the hydrophilic groups of the polymer, but non-freezing water is stronger than intermediate water. However, the intermediate water can be accumulated like a shell and observed as tightness layers around hydrophilic groups of the polymer. This association is due to the natural phenomenon of (ion) solvation. Finally, the excess water molecules are surrounded the hydration shell and can be defined as free water which is almost surplus to the requirement of solvation [29–31]. The free water is related to the three-dimensional structure and pore volume of the hydrogel as it is physically entrapped within the hydrogel networks. It has a very high degree of freedom (does not take part in interaction with polymer chains), leading to easy

mobility and dehydration. Consequently, the water retention with different time presented water evaporation after the hydrogels have been fully swollen and occurred by losing the free water molecules. The water retention as a function of time, for each Na-AMPS and PCL diol hydrogel composition with various concentrations of PEGDA crosslinker, is shown in Fig. 7. The evaporation rates reached equilibrium over 48 h, however the profiles varied according to concentration of the PEGDA crosslinker and ratio of Na-AMPS to PCL diol. The equilibrium water retention (*EWR*) is shown in Fig. 6b, demonstrating that at equilibrium some free water is retained along with bound water.

From Fig. 7, the water retention-time profile for the different ratios of Na-AMPS and PCL diol with varying PEGDA crosslinker concentrations shows that the water evaporation rate slows and reaches equilibrium at different times. The results show that the higher PEGDA content shows a faster rate of water evaporation. A lower crosslinking degree enables a higher water-uptake capacity, resulting in increased free water content thus a slower rate of water loss. Furthermore, an increase in PEGDA content leads to a significant increase in *EWR* (Fig. 6b). This is because PEGDA is a hydrophilic polymer and an increase in PEGDA contributes to an increase in the overall hydrophilicity of the hydrogel. There is thus an increased interaction between hydrophilic groups on polymer chains with water molecules via hydrogen bonding. The increase in bound water within the network structure, leads to a higher *EWR* and in turn improves the ability hydrogel of the to retain moisture.

The effect of varying Na-AMPS and PCL diol composition, on water evaporation at different time intervals, demonstrated that the hydrogels consisting of both Na-AMPS and PCL diol exhibit a slightly slower rate of water evaporation compared to pure P(Na-AMPS) hydrogel. This can be explained in terms of an outer “skin” layer forming on the outermost region of the hydrogel. Hydrophobic interactions amongst the hydrophobic groups in the outermost region become stronger with evaporation. This results in rapid shrinkage of the outermost surface and the formation of a dense layer of hydrogel skin. Once this skin layer is formed, the free water molecules in the hydrogel structure are prevented from moving out, and this results in a slow evaporation response rate [7]. It can be seen in Fig. 6b that at equilibrium, the semi-IPN hydrogel containing PCL diol at 10 %w/$w_{Na\text{-}AMPS}$ has lower *EWR* values compared to pure P(Na-AMPS) hydrogel (PCL diol at 0 %w/$w_{Na\text{-}AMPS}$). This result can be explained in terms of PCL diol preventing network structure creation within the hydrogel, resulting in larger pore sizes and an apparent reduction in crosslink density, so free water molecules evaporate easily. An increasing amount of PCL diol (> 10 %w/$w_{Na\text{-}AMPS}$) slightly

increased EWR as shown in Fig. 6b. The PCL diol is considered as a hydrophobic layer in the outermost of hydrogel surface to hamper the water escaping from the hydrogel. With an increase of the content of PCL diol over 10 %w/$w_{Na\text{-}AMPS}$ in the hydrogels, the hydrophobic layers in the network increased, the hydrogel became harder to lose water.

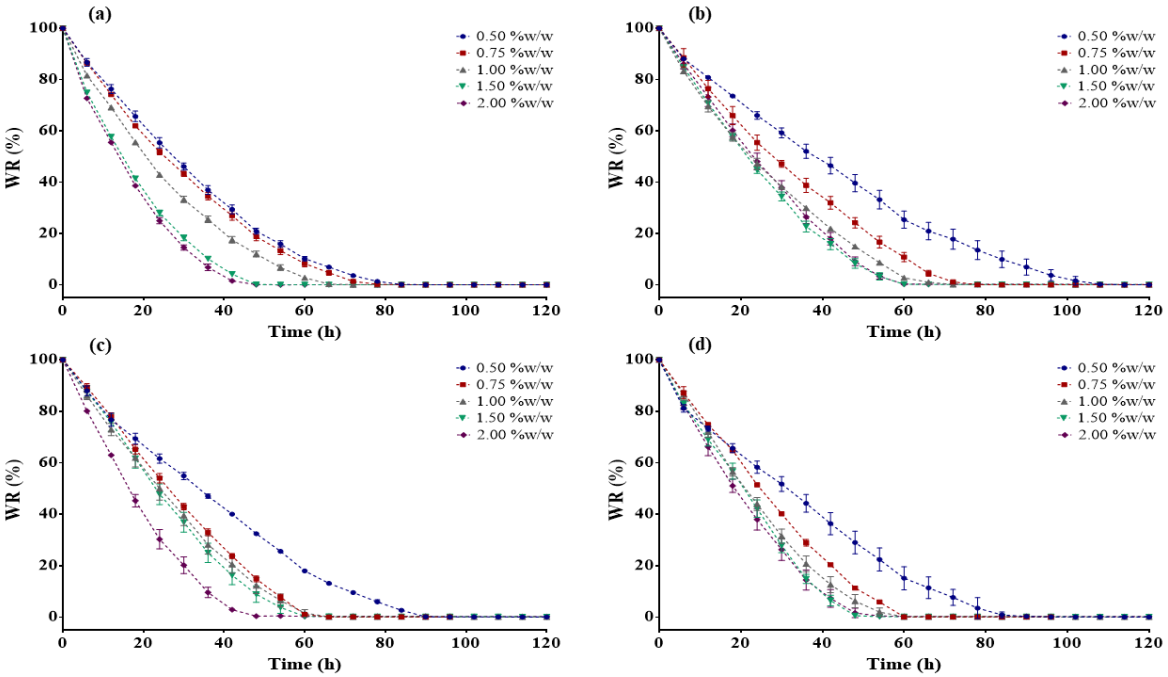

Fig. 7. The water retention-time profile of hydrogel in different concentration of PEGDA crosslinker (0.50 - 2.00 %w/$w_{Na\text{-}AMPS}$) with various concentrations of PCL diol at (a) 0, (b)10, (c) 30 and (d) 50 %w/$w_{Na\text{-}AMPS}$.

3.5 Mechanical properties by tensile testing

In this series of experiments, the mechanical property was investigated as a function of the ratio of Na-AMPS and PCL diol with various concentrations of PEGDA crosslinker, as shown in Fig. 8. The mechanical property of hydrogel was studied in terms of tensile strength, elongation at break and Young's modulus, which were found to range between 9.8 - 70.1 kPa, 116.1 - 517.6 % and 0.02 - 0.66 kPa respectively.

The results shown in Fig. 8 show that Young's modulus and tensile strength of hydrogels increased as PEGDA crosslinker content increased. In contrast, the elongation at break decreased with increasing crosslinker concentration. This behavior can be explained in terms of an increased network crosslinking density. This increase restricts the motion of the

chains, generally resulting in a decrease in the flexibility and toughness of the hydrogel enhancing its rigidity, stiffness and brittleness.

The incorporation of PCL diol into the Na-AMPS network significantly influenced the mechanical properties of the resulting hydrogels. With increasing PCL diol content, Young's modulus and tensile strength of the synthesized hydrogels decreased, similar to other work [32]. Na-AMPS is a hydrophilic polymer whilst PCL diol consists of a hydrophobic microcrystalline core. This data suggested that the increased concentrations of PCL diol lead to hydrophobic aggregation within the Na-AMPS network. In turn, such aggregates delay or completely prevent Na-AMPS crosslinking, which could result a weakened microstructure and obtained the low elastic modulus. However, a unit of PCL diol molecule has five methylenes that bestow good flexibility. Compared to the hydrogel without PCL diol, the elongation at break of the hydrogels containing PCL diol tends to increase with increasing PCL diol content. The hydrogel without PCL diol exhibits typical brittle fracture failure. With increasing PCL diol percentage to 50 %w/$w_{Na\text{-}AMPS}$, the hydrogel is transformed from brittle to flexible. This result agrees well with the previously reported work and confirms that incorporating PCL diol can improve the flexibility of the semi-IPN hydrogels [33].

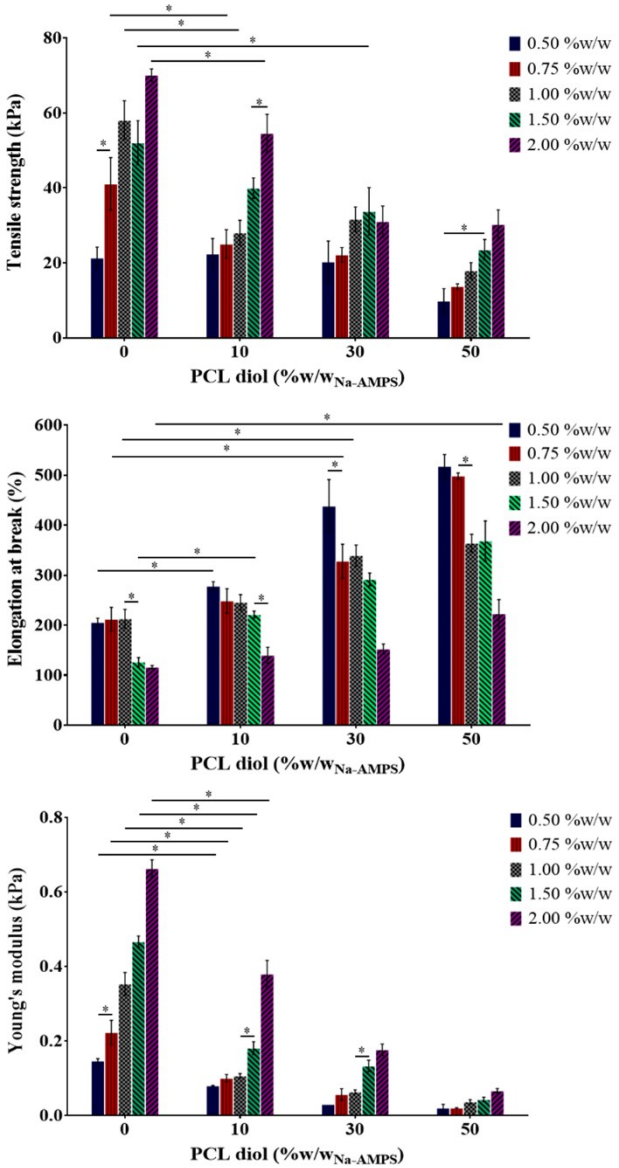

Fig. 8. The mechanical properties of the hydrogels for different compositions of Na-AMPS and PCL diol at various PEGDA crosslinker content (* $p < 0.05$).

In summary, so far, the results indicated that an increasing of crosslinker concentration resulting a decrease in water uptake of hydrogels, increased stiffness and reduced elasticity. This is due to hydrogels with a higher crosslinker concentration display greater resistance to expansion of hydrogel matrix, decreasing the free volume within the hydrogel and therefore resulting in reduced water absorption and elasticity. Thus, the different of crosslinker concentrations are an effective way of controlling the properties of water transport and mechanical of the hydrogel. For balanced water transport and mechanical properties, PEGDA crosslinker at 0.75 %wt of Na-AMPS was deemed an appropriate crosslinker concentration with different Na-AMPS and PCL diol ratios. These findings demonstrate the importance of

finding the suitable balance between monomer composition and crosslinker concentration when designing a hydrogel to be employed as a drug delivery material.

3.6 SEM analysis

The presence of pores plays an essential role in the properties of hydrogels, such as swelling [34], nutrient diffusion [35], cell adhesion [36] and compressibility [37]. Pores are physical structures in the hydrogel network through which water molecules can easily diffuse. Consequently, porous hydrogels have efficiency applications in the controlling of drug-release due to the porous network may provide enough space for the loading and release of drugs and it also enables fluid absorption when used as an absorbent [7]. The pores were a result of ice crystal formation during the freeze-dried process to prepare hydrogels before SEM analysis [38]. Consequently, the water molecules in the hydrogel structure which is the equilibrium swollen state were frozen into smaller ice crystal and then, these ice crystals were eventually represented by smaller pores.

The surface and cross-section morphologies of freeze-dried swollen hydrogels were observed using SEM as illustrated in Fig. 9. The surface morphology of hydrogels with different ratios of Na-AMPS and PCL diol showed a homogeneously porous morphology and exhibited no phase separation on the hydrogel surface. The surface of the semi-IPN hydrogel containing PCL diol at 50 %w/$w_{Na\text{-}AMPS}$ was presented rough and also showed smaller pore size than that of the single P(Na-AMPS) hydrogel, but the porosity distribution became regularly and more thickly.

In addition, the microphotographs of the cross-section for all hydrogels show evidence of the porous three-dimension structure which confirms the interconnection between the pores as a result of the crosslinking semi-IPN formation within the hydrogels. However, it also indicated that the Na-AMPS and PCL diol did not parent any physical incompatibility within the hydrogel network. The images clearly illustrated the internal morphology is dependent on the composition ratio of PCL diol to Na-AMPS. The hydrogel without PCL diol has the largest pore size, while hydrogel containing PCL diol at 50 %w/$w_{Na\text{-}AMPS}$ has the smallest. This trend may explain the water uptake of the hydrogels discussed above. An increasing of the PCL diol content, the hydrophilicity of the hydrogel network decreases, and the crosslink density increased (Section 3.7), which resulted in the decrease in water uptake (Section 3.3) and limited water transport. A similar trend was observed for prepared hydrogel from PCL and acrylic acid in the previously reported study. They reported porosity was decreased on increasing PCL

concentration [11]. Furthermore, the SEM images of the hydrogels containing PCL diol was illustrated ductile fractures, indicating a flexible network. This observation is in tandem with the tensile testing of the hydrogels discussed in Section 3.5. This result also indicates that the flexibility of the hydrogels can be tailored by changing the composition ratio of PCL diol to Na-AMPS.

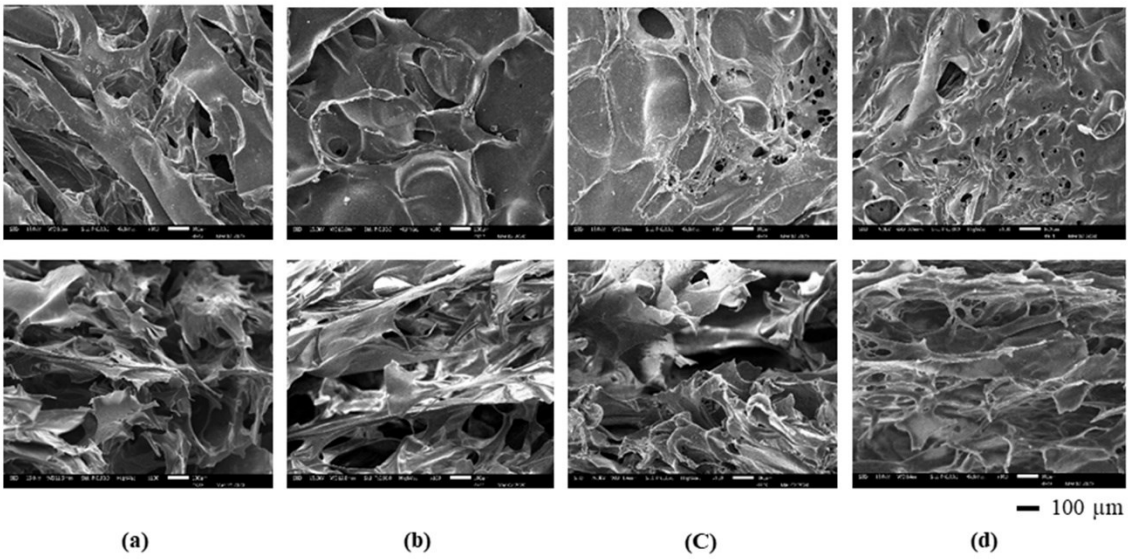

Fig. 9. SEM images at magnification ×100 of the surface (upper row) and the cross-section (lower row) of hydrogels at constant PEGDA 0.75 %w/$w_{Na\text{-}AMPS}$ with varying PCL diol concentration of (a) 0, (b)10, (c) 30 and (d) 50 %w/$w_{Na\text{-}AMPS}$.

3.7 Crosslink density

The approaches used to determine the crosslinking degree of polymer networks, include the evaluation of stress-strain data or tensile measurements (Section 3.5) and use of equilibrium water uptake experiments (Section 3.3). Tensile experiment fails to consider the effect of physical crosslinks, i.e., chain entanglements, due to these may be disentangle during extension by tensile force. This destroy of physical entanglement process does not occur with experiment of water uptake. Generally, the water uptake is influenced by the crosslinking density and the overall hydrophilicity of the resulting hydrogel. So, experiment of water uptake was evaluated the crosslink density of hydrogels more accurately due to including the effects of the physical entanglement present [39].

The crosslink density (*XD*) of P(Na-AMPS)/PCL diol semi-IPN hydrogels were evaluated using the Flory-Rhener theory [40,41] and presented in Fig. 10. It was found that the semi-IPN hydrogel containing different concentrations of PCL diol (0, 10, 30, and 50 %w/$w_{Na\text{-}AMPS}$) with PEGDA 0.75 %w/$w_{Na\text{-}AMPS}$ were calculated between the range of 5.6×10^{-5} to 11.8×10^{-5}. The PCL diol content influenced the *XD*. The single P(Na-AMPS) hydrogel showed greater crosslink density compared to the semi-IPN hydrogel, this is due to PCL diol aggregation preventing complete crosslinking of Na-AMPS, thus leading to a looser network. However, increasing PCL diol from 10 - 50 %w/$w_{Na\text{-}AMPS}$ ensued in an increased, this could mainly be due to the evidenced increase hydrophobic interaction of PCL diol resulting high physical crosslinking point in hydrogel network as agree with Danafar, H. et al. [28].

The *XD* values were influenced by PCL diol content and the same trend coincided with the calculated values of tensile strength. Consequently, the remarkable decrease in tensile strength of the semi-IPN hydrogels is due to the dramatic decrease in crosslink density compared to the single component hydrogel. This characteristic, together with the comparatively lower tensile strength properties of semi-IPN hydrogels, could be highly advantageous in developing drug delivery systems for biomedical applications [32].

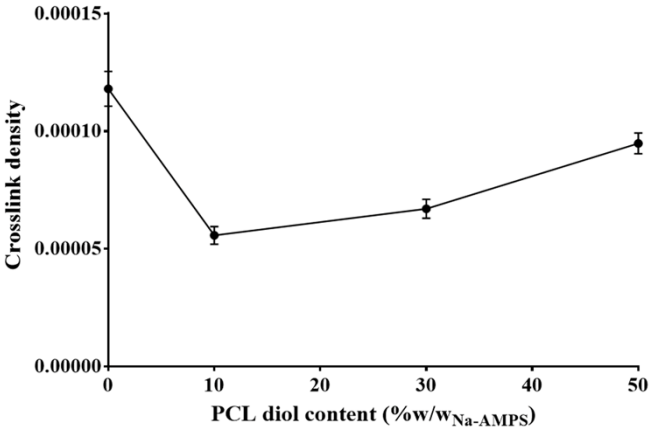

Fig. 10. The crosslinking density of hydrogel at constant PEGDA 0.75 %w/$w_{Na\text{-}AMPS}$ with different PCL diol contents.

3.8 Evaluation of cytotoxicity

Cytotoxicity assays are used to investigate in vitro biocompatibility and serve as a preliminary cytotoxicity evaluation of new medical devise and biomaterials for possible

biomedical applications. In this study, the cell viability of the hydrogels on L929 mouse fibroblast cells was measured by the MTT method. This method is widely accepted as a short time and accurate test for cell proliferation rate and conversely the cellular viability reduction when metabolic events resulting apoptosis or necrosis. The average percentage of cell viability of all hydrogels is shown in Fig. 11. The negative control was 'Thermanox' (Nunc) coverslip. The cell viability of all hydrogels was higher than 85% after incubation for 24 h. According to ISO 10993-5 for MTT cytotoxicity assay, a material stimuluses cytotoxic effects when it causes reduction in cell viability greater than 30% [42]. The results indicated that the hydrogel in this research with various compositions was considered non-cytotoxic to L929 cells. Therefore, all samples were non-toxic and are deemed to have good biocompatibility for biomedical applications such as drug delivery, tissue engineering, and biomedical implantations [43].

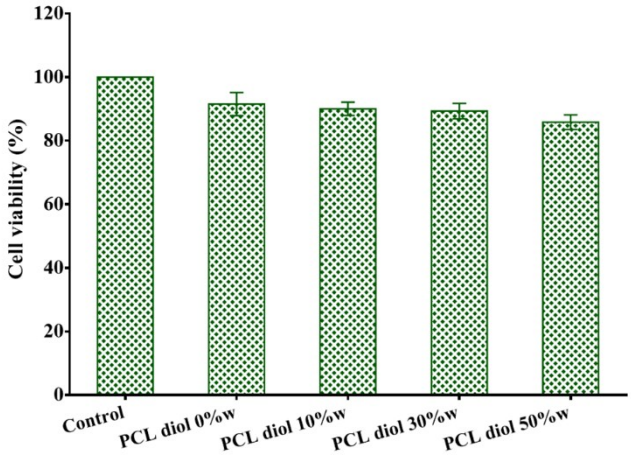

Fig. 11. Cytotoxicity test of hydrogels at constant PEGDA 0.75 %w/$w_{Na\text{-}AMPS}$ with different PCL diol contents ($p > 0.05$).

3.9 Drug loading and entrapment efficiency

Drug can be incorporated into hydrogel networks in two methods: 1) post-loading and 2) in-situ loading during synthesis. The post-loading diffusion method was chosen to load ciprofloxacin (CIP) in hydrogels. This was to minimize potential changes to the structure and properties of CIP that may occur if incorporated during synthesis. In addition, the loading method has an impact on the release of CIP. Based on experience, the diffusion method is preferred [44]. In this study, dried hydrogels with varying ratios of Na-AMPS and PCL diol were immersed into aqueous solutions of CIP at 0.05, 0.15 and 0.25 mg/ml.

The effect of the ratio of Na-AMPS and PCL diol with different CIP concentrations on entrapment efficiency (EE) and drug loading (DL) were studied, and the results are tabulated in Table 1. The values of EE and DL were calculated according to the CIP standard curve (A = 100.33C + 0.0242, r^2 = 0.9992, linear range, where A is Absorbance and C is concentration). As shown in Table 1, EE of these hydrogels is > 99% (not significantly different, $p > 0.05$) with DL values varying in the range of 1.04 to 6.36 % (w/w to hydrogel). Compared with single P(Na-AMPS) hydrogel, the DL of all semi-IPN hydrogels is higher and the maximum was obtained with PCL diol at 50 %w/$w_{Na\text{-}AMPS}$. The amount of CIP loaded by hydrogels increased with the increase of PCL diol content. Interactions by hydrogen bond between the semi-IPN hydrogel functional groups and CIP encapsulate more drug as a result of greater binding affinity, resulting in higher drug loading [45]. Furthermore, at higher initial CIP concentration, the drug loading level of hydrogels was greater than that of the lower CIP concentration.

3.10 In vitro drug release study

The ultimate aim of this research was to investigate the ability of the P(Na-AMPS)/PCL diol semi-IPN hydrogels to act as a matrix for drug release systems. The *in vitro* drug release profile (CIP as a model drug) was studied for the semi-IPN hydrogel containing different concentrations of PCL diol (0, 10, 30, and 50 %w/$w_{Na\text{-}AMPS}$) with PEGDA 0.75 %w/$w_{Na\text{-}AMPS}$, which demonstrated the most appropriate properties (Section 3.5). The CIP release from P(Na-AMPS)/PCL diol semi-IPN hydrogels was investigated in PBS of pH 7.4 at 37.0 ± 1.0 ℃, which mimicked the environment of healthy tissues. Meanwhile, the hydrogen bonds between the semi-IPN hydrogels and the CIP molecules were weakened at 37 °C, so that the CIP molecule, which is encapsulated in the hydrogel's interior, can diffuse more easily into the release medium [46]. Figure 12 shows the drug release profile of the CIP-loaded hydrogels at 37.0 ± 1.0 °C in PBS (pH 7.4). It was found that the hydrogel was shown rapid in the initial release and then reach equilibrium with different times. The maximum percentage cumulative drug release and time at equilibrium were summarized in Fig. 13, which are depended on PCL diol and CIP concentration.

An increase in the concentration of PCL diol decreased the maximum percentage release. Due to the release of drugs and water uptake of hydrogels are directly proportional to each other. The high water uptake resulted in more drug diffusion from the hydrogel [47]. These depended on the mesh size of the polymer network, which commonly decrease water

uptake and drug release with the increasing crosslinking network. In this case, PCL diol can be presented the physical crosslinking by forming of the polymer-polymer hydrophobic interaction. In addition, the hydrogen bonds between CIP and hydrogels are still capable of retaining much-loaded drugs lead to low drug releasing. As illustrated Fig. 14, these results are the hydrogen bonding between the carboxylic group in the CIP and the amide-II group on the Na-AMPS structure. In particular, the presence of the hydroxyl end-groups and carbonyl groups of repeating units on the PCL diol structure suggests strong hydrogen bonding with the carboxylic group in the CIP. The results were lead to the restraining effect on drug releasing which confirmed that the high PCL diol resulting low values of percentage release.

For hydrogels soaked in different CIP concentrations, an increasing the CIP concentration with the maximum percentage release was decreased. Consequently, the higher the drug loading, the lower the rate of release and the lower the rate of drug utilization. Most of the drug molecules concentrate near the hydrogel surface were released by diffusion along with the medium. At the hydrogel-release medium interface, the different concentrations drive occurred. The drug molecules at the hydrogel surface favor the release medium. This causes an “imbalance” at the hydrogel surface and thus drug molecules are drawn to the hydrogel surface. This process is slow when the concentrations within the hydrogel and at the surface reaches an equilibrium.

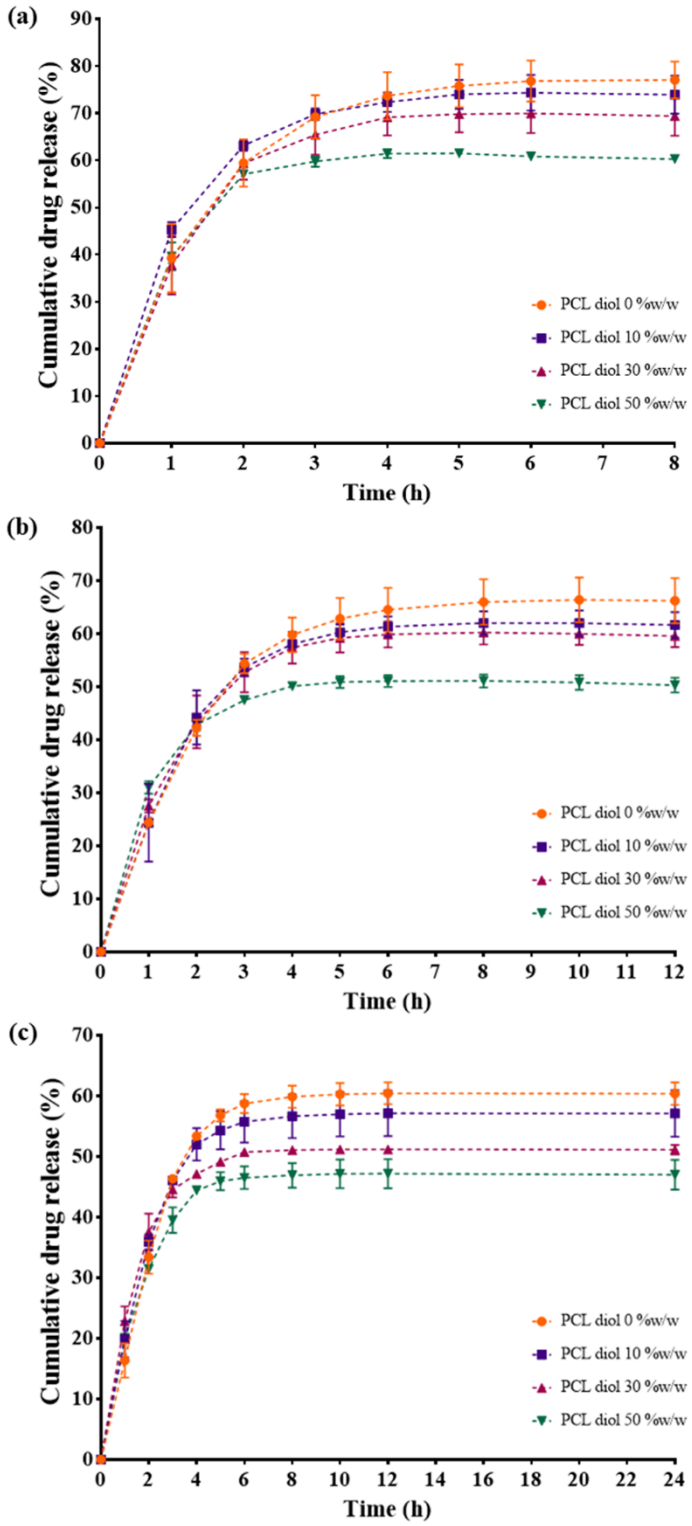

Fig. 12. Comparison of *in vitro* drug release of CIP from hydrogels with different PCL diol contents by loading CIP at (a) 0.05, (b) 0.15 and (c) 0.25 mg/ml.

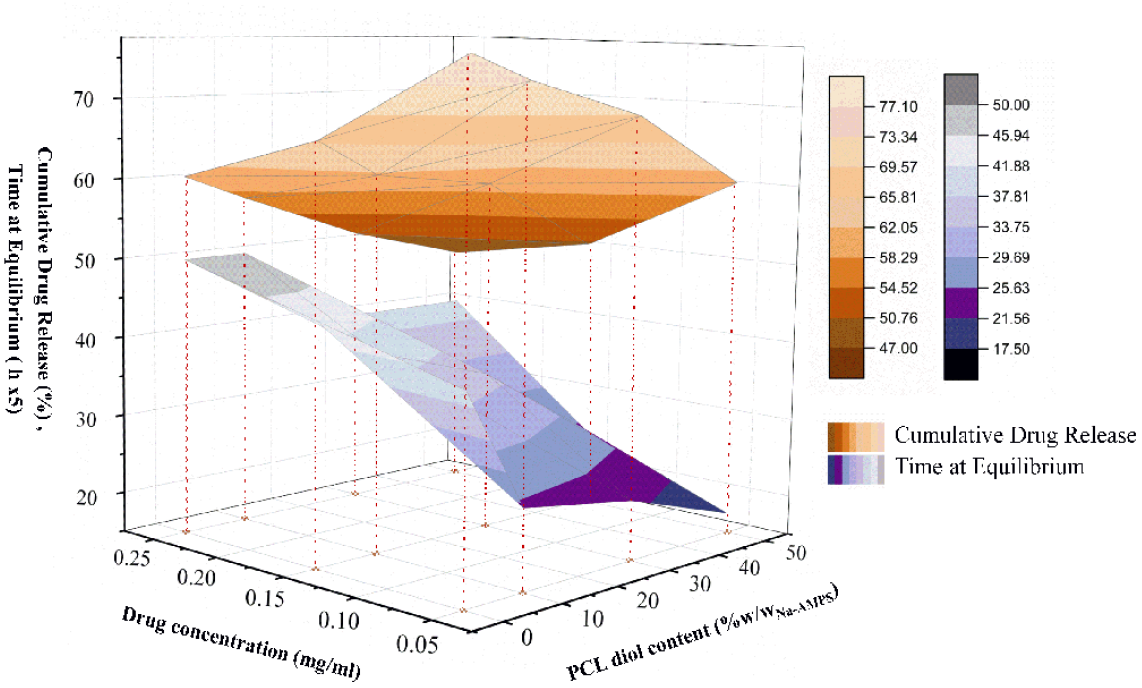

Fig. 13. The maximum percentage cumulative drug release and time at equilibrium in function of hydrogel composition and drug content.

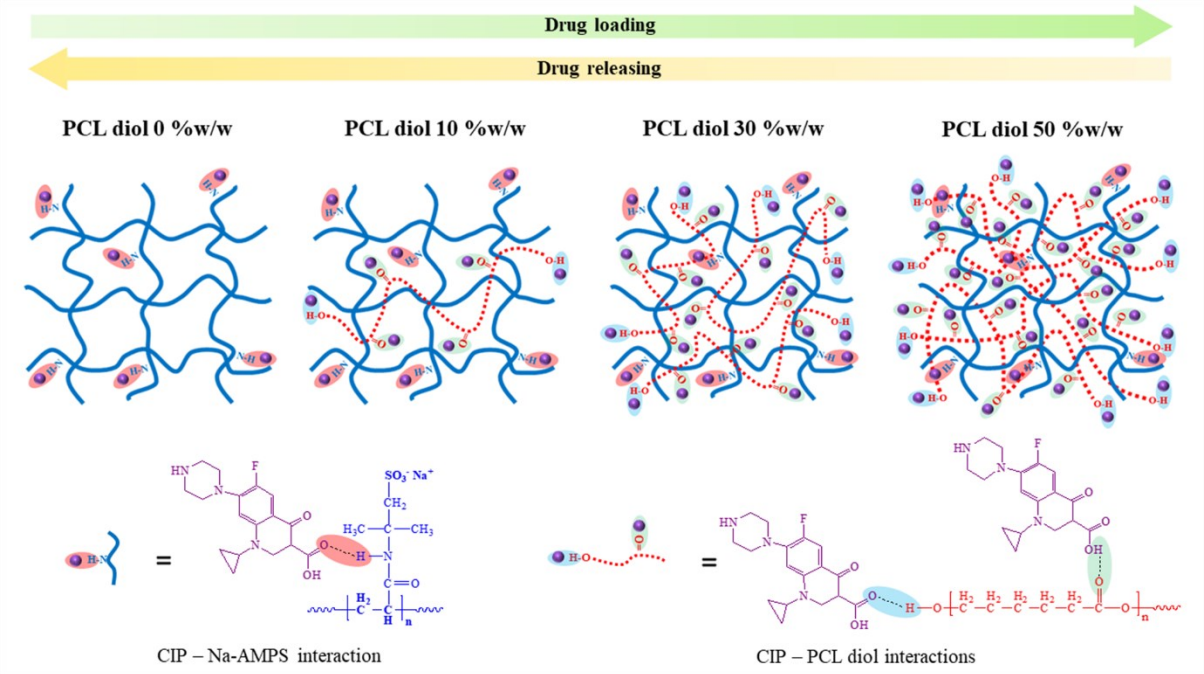

Fig. 14. Illustration of CIP-hydrogel interactions effect on the drug-releasing compared with different PCL diol contents.

3.11 Analysis of the drug transport mechanism

In a hydrogel system, the water absorption from the surrounding media was resulted to change the dimensions and physical-chemical characteristics of the hydrogel. Such changes promote drug release from a hydrogel substrate. Generally, drug release occurs due to enlargement of the mesh and network loosening as a result from the degradation and swelling of the hydrogel matrix. Rezk, A. I. et al. [48] reported that the process of drug release can be explained as a three-step process. First, hydrated hydrogel occurs through absorption of the dissolution media into the hydrogel structure. Second, polymer relaxation or erosion occurs. During this process, the hydrogel changes from a glassy state to a rubbery state due to mobility polymer chains. This case is called relaxation of the hydrogel. At equilibrium swelling state, the elasticity forces of the chain crosslinks are balanced with the osmotic forces of the solvent. However, the osmotic forces are more than the elasticity forces, resulting in the degradation of the hydrogel and leading to the dissolving of small fractions. This process is called the erosion of the hydrogel [49]. In the third step, the dissolved drug transfers either through from the hydrated hydrogel or the eroded part of hydrogel to the surrounding dissolution medium. Moreover, Ghasemiyeh, P. et al. reported that the controlled mechanism of drug release from hydrogel can be divided into three categories: diffusion-controlled, swelling-controlled and polymer-degraded release [50]. However, these mechanisms are described by the *n* values from the Korsmeyer-Peppas model. If $n < 0.5$ the drug release mechanism is pseudo Fickian diffusion (diffusion-controlled release); $n = 0.5$ the mechanism is Fickian diffusion; $0.5 < n < 1$ the drug release mechanism is non-Fickian diffusion or anomalous diffusion coupled with relaxation or swelling of hydrogel matrix (swelling-controlled release). Once the *n* value reaches 1 and above, the release can be characterized by non-Fickian diffusion, this is essentially drug release by erosion of hydrogel matrix (polymer-degraded controlled) [51,52].

Consequently, drug release kinetics and mechanism were studied for the prepared hydrogels in this research. To evaluate the kinetics of drug release, five different mathematical models (e.g., zero-order, first-order, Higuchi, Korsmeyer-Peppas, and Hixson-Crowell) were applied to drug release data. Drug release data plotted to various kinetic models show in Fig 15, S1 and S2, and kinetic parameters are expressed in Table 1. These values provide an indication of the drug transport mechanism. The suitable kinetic model for each hydrogel was considered by determining the highest degree of correlation coefficient (r^2) to symbolize drug release behavior. It was found that the CIP release from hydrogels revealed a very high r^2 with the Higuchi and Korsmeyer-Peppas model. Therefore, it could be said that the drug release

mechanism can be explained with both of two mathematical model and details was described below.

The Higuchi model is used to describe the release of water-soluble or low solubility of drug. It is distributed within the porous matrix which is insoluble and swellable in the medium. It is based on the hypothesis that the drug initial concentration in the hydrogel matrix is higher than the drug solubility. The drug is dissolved and diffused evenly exit to solvent medium. At the same time, the matrix is negligible swelling occur [53]. Furthermore, the *n* values calculated with the Korsmeyer-Peppas model to determine the CIP release mechanisms of hydrogels are provided in Table 1. The *n* values of CIP release from hydrogel indicate that excluding the hydrogels containing PCL diol at 0 and 10 %w/$w_{Na\text{-}AMPS}$ loaded with 0.15 and 0.25 mg/ml CIP was released according to Fickian diffusion law. With the Fickian diffusion mechanism, *n* values are less than 0.50, and release is controlled by the diffusion rate of water into the hydrogel. For hydrogel containing PCL diol at 0 and 10 %w/$w_{Na\text{-}AMPS}$ loaded with 0.15 and 0.25 mg/ml CIP, the drug release behavior followed non-Fickian anomalous transport with *n* values in the 0.5 - 1.0 range. This suggests that drug diffusion through the matrix occurred simultaneously with matrix relaxation or swelling. Thus, the drug release mechanism of hydrogel in PBS solution was performed according to diffusion and swelling of hydrogel matrix (Fig. 16) when *n* diffusion exponent was examined, dependent on PCL diol and CIP concentration.

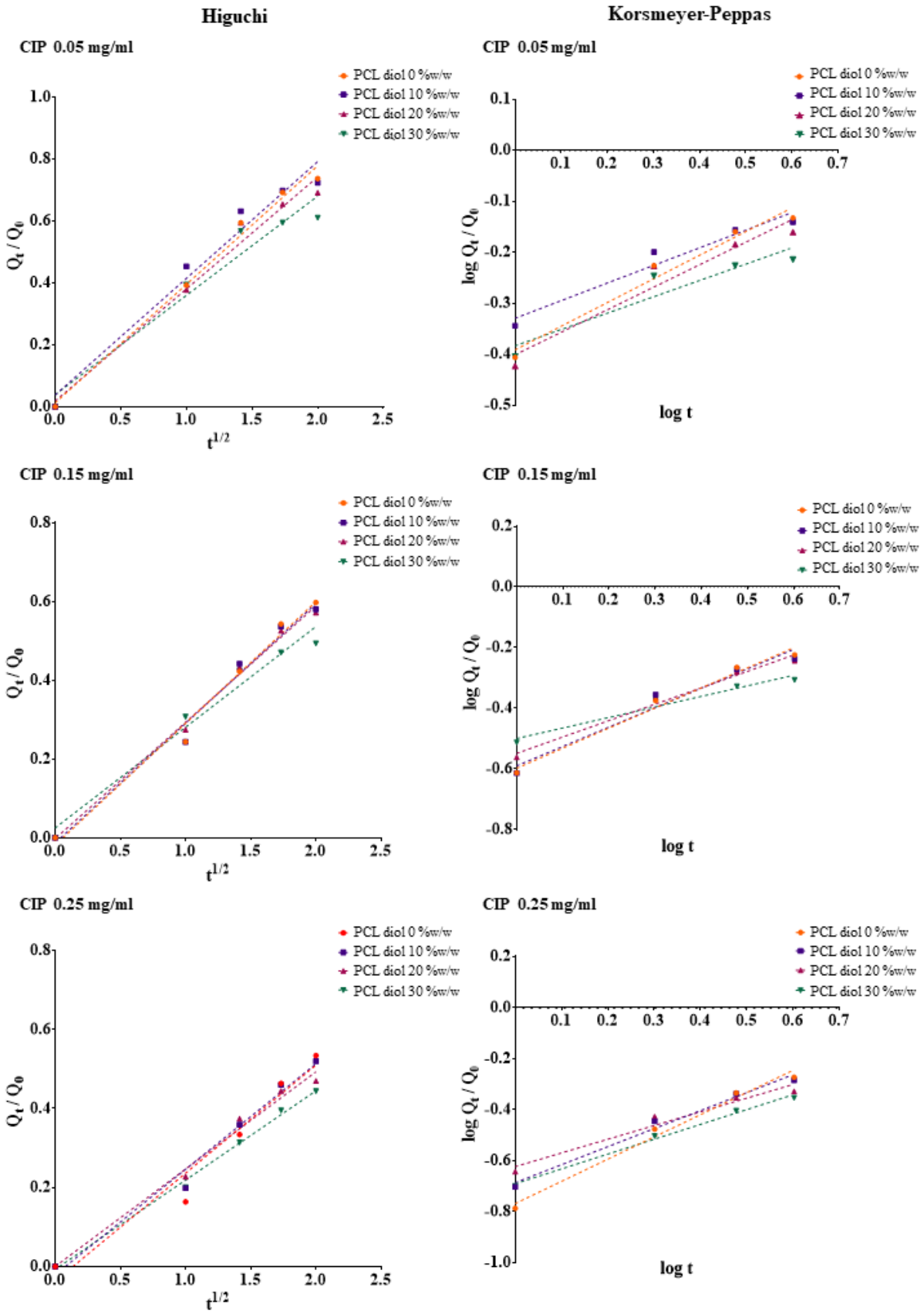

Fig. 15 The Higuchi (left) and Korsmeyer-Peppas (right) model for hydrogel with different PCL diol contents by loading CIP of 0.05, 0.15 and 0.25 mg/ml.

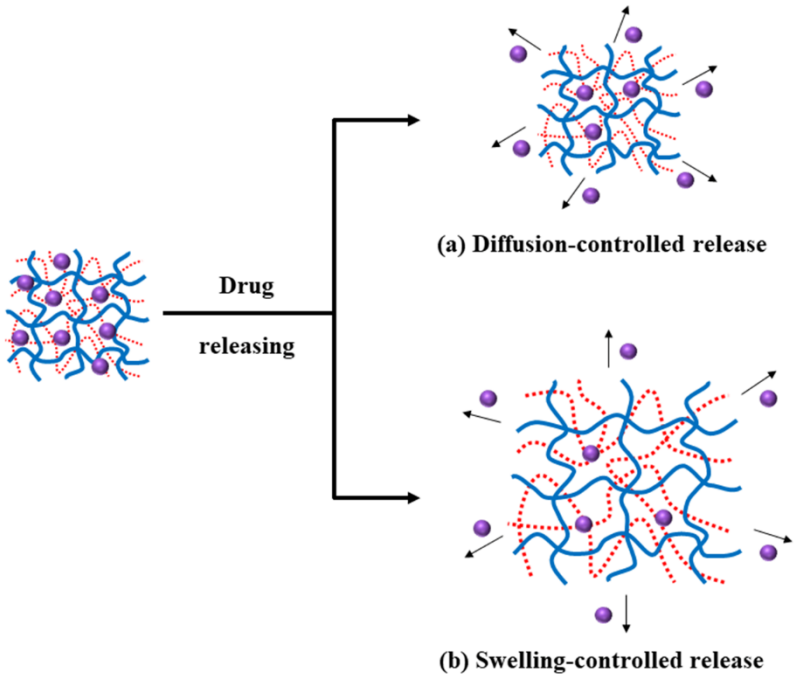

Fig. 16. Mechanism of drug release from hydrogels.

Table 1 shows that the First-order kinetic model presented low values of r^2 in the range of 0.738 to 0.924, suggesting that this model did not suitably describe the CIP transport in hydrogels. This is due to this model is used to describe the characteristic of porous matrix containing good water-soluble drugs. However, CIP is a sparingly water-soluble drug which is reported to be 0.086 - 0.22 mg/ml [53,54]. According to the zero-order kinetics and Hixson-Crowell models, it can be explained that the drug release mechanism of the hydrogel caused by surface erosion [55]. It was also found that the drug release mechanism of the hydrogel in this research did not follow zero-order (r^2 = 0.764 - 0.978) and Hixson-Crowell (r^2 = 0.607 - 0.777) model. So, it can confirmed that the drug release mechanism was more consistent with a diffusion and relaxation mechanism than a matrix erosion mechanism.

Table 1 Release kinetic and mechanism of CIP release from hydrogels (* $p > 0.05$).

CIP concentration (mg/ml)	PCL diol (%w/$w_{Na\text{-}AMPS}$)	EE (%) *	DL (%)	Zero-order		first-order		Higuchi		Korsmeyer-Peppas			Hixson-Crowell	
				r^2	k_0	r^2	k_1	r^2	k_H	r^2	k_{KP}	n	r^2	k_{HC}
0.05	0	100.00±0.00	1.04±0.05	0.869	0.177	0.865	-0.204	0.990	0.383	0.969	0.406	0.464	0.659	-0.109
	10	100.00±0.00	1.07±0.04	0.798	0.169	0.828	-0.150	0.968	0.377	0.949	0.469	0.346	0.619	-0.107
	30	99.96±0.02	1.41±0.04	0.841	0.166	0.804	-0.191	0.978	0.362	0.933	0.397	0.442	0.647	-0.107
	50	99.46±0.07	1.48±0.13	0.764	0.142	0.738	-0.136	0.950	0.321	0.886	0.414	0.320	0.607	-0.100
0.15	0	99.95±0.05	2.59±0.16	0.943	0.149	0.892	-0.294	0.986	0.309	0.997	0.253	0.600	0.721	-0.141
	10	99.94±0.03	2.65±0.10	0.921	0.145	0.846	-0.280	0.983	0.304	0.989	0.257	0.570	0.708	-0.139
	30	99.76±0.17	3.59±0.12	0.907	0.140	0.890	-0.240	0.994	0.296	0.997	0.283	0.502	0.685	-0.137
	50	99.85±0.31	3.75±0.05	0.805	0.115	0.851	-0.152	0.972	0.256	0.979	0.317	0.314	0.621	-0.126
0.25	0	99.95±0.04	4.01±0.06	0.978	0.137	0.900	-0.387	0.957	0.274	0.997	0.171	0.622	0.777	-0.165
	10	99.88±0.07	4.10±0.02	0.954	0.130	0.895	-0.314	0.983	0.267	0.999	0.206	0.538	0.733	-0.160
	30	99.56±0.08	6.00±0.45	0.889	0.116	0.844	-0.235	0.988	0.246	0.983	0.238	0.413	0.679	-0.152
	50	99.85±0.06	6.36±0.49	0.933	0.108	0.924	-0.261	0.996	0.226	0.998	0.204	0.407	0.701	-0.149

3.12 In vitro hydrolysis degradation analysis

One of the critical factors contributing to the wide use of hydrogels in different applications, for example medical applications complementary to tissue engineering, such as wound dressing, scaffolds and dentistry, is its degradability. As far as drug delivery materials are concerned, the degradation of hydrogels is essential.

The in vitro degradation of hydrogel with different Na-AMPS and PCL diol compositions was studied, and the result is shown in Fig. 17. A degradation behavior study was performed by immersing the hydrogels in PBS solution (pH 7.4) at 37.0 ± 1.0 ℃ for 168 days. It was noted that the hydrogel containing PCL diol has a higher percentage degradation compared to that of the hydrogel without PCL diol. The result may be explained in terms of the degradation of hydrogels occurring due to hydrolysis of the PCL diol ester bonds, which allow the release of PCL microparticles from the hydrogels into the surrounding media. Moreover, it can be explained by the mechanical properties. The hydrogel containing PCL diol has a lower tensile strength and higher elongation at break than the hydrogel without PCL diol, resulting in low stability. This result can be interpreted in terms of increased network chain extensibility which allows water molecules to diffuse more easily into the network. This increased the probability of catching a water molecule with a PCL diol polymer chain, resulting in the formation of PCL diol microparticles and falling out. However, increasing a large amount of PCL diol resulted in the hydrogel water uptake decreasing slightly, but with no significant difference in degradation. The water uptake and mechanical properties of Na-AMPS/PCL diol hydrogel are shown in sections 3.3 and 3.5 respectively.

The percentage degradation of the hydrogels is in the range of 4.1×10^{-4} to 12.1×10^{-4} %, which is less than 0.1 %. This suggests that the hydrogel was very stable when immersed in PBS (pH 7.4) at 37 ± 1.0 ℃. The degradation mechanisms of hydrogels are relevant in drug release applications, as they strongly affect the kinetics of the release (refer to the results of the above-mentioned kinetic studies in Section 3.11).

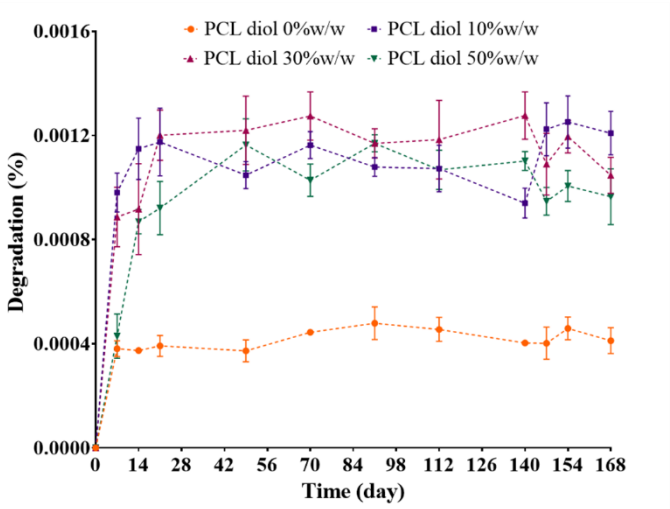

Fig. 17. The percentage degradation-time profile of hydrogels at constant PEGDA 0.75 %w/$w_{Na\text{-}AMPS}$ with different PCL diol contents.

4. Conclusion

The primary intention of the present work was to synthesize semi-IPN hydrogel from Na-AMPS and PCL diol with PEGDA as a crosslinker for sustained release of antibiotic ciprofloxacin (CIP) as a model drug. The hydrogel structure was studied by FTIR and SEM techniques. To investigate the effect of PEGDA concentration on the hydrogel properties, the (Na-AMPS)/PCL diol semi-IPN hydrogels were synthesized with various crosslinker concentrations (ranging from 0.50 to 2.00 %wt of Na-AMPS). By adjusting the concentration of PEGDA crosslinker, the properties of the synthesized hydrogels were controlled precisely: including, swelling, water retention, and mechanical properties. It was shown that the PEGDA crosslinker at 0.75 %wt of Na-AMPS is an appropriate concentration for the semi-IPN hydrogel, as it provided balanced water transport properties and mechanical properties desired by hydrogels for use in drug delivery applications. The effect of PCL diol content (ranging from 0 to 50 %wt of Na-AMPS) on various hydrogel properties was also evaluated. It was found that the hydrogel containing PCL diol at 10 %w/$w_{Na\text{-}AMPS}$ had a high water uptake at equilibrium but a lower equilibrium water retention. Increasing the amount of PCL diol above 10 %w/$w_{Na\text{-}AMPS}$ slightly decreased the water uptake at equilibrium, but increased the equilibrium water retention. Thus, PCL diol is seen to play an influential role in enhancing hydrogel elasticity and adjusting the biodegradation rate. These results are considered to be advantageous for a semi-IPN hydrogel.

For the preparation of a semi-IPN hydrogel incorporating CIP, the CIP was incorporated into the semi-IPN hydrogel by a swelling-diffusion approach. The influence of PCL diol and CIP content was studied. CIP loading efficiency was significantly enhanced by the presence of PCL diol, which confirms that a semi-IPN hydrogel can improve drug loading. Furthermore, loading efficiency was affected by the initial concentration of CIP which increased loading efficiency with increasing initial concentration of CIP. Five kinetic models were calculated to evaluate the drug transport mechanism of the semi-IPN hydrogel. It was found that the drug-release profile could be fitted to the Higuchi and Korsmeyer-Peppas models. The drug release mechanism followed Fickian and non-Fickian diffusion which is diffusion- and swelling-controlled releases, depending on the PCL diol and CIP concentration. The overview of properties relationships in function of hydrogel composition was demonstrated in Fig. 18. In addition, the prepared hydrogels were shown to be non-cytotoxic as confirmed by MTT assay studies. This demonstrated the potential for these hydrogels to be used as an efficient biomaterial for the drug delivery. Consequently, this study will be served as a platform in the design and development of novel controlled drug delivery system with improved drug loading capacity and sustained release.

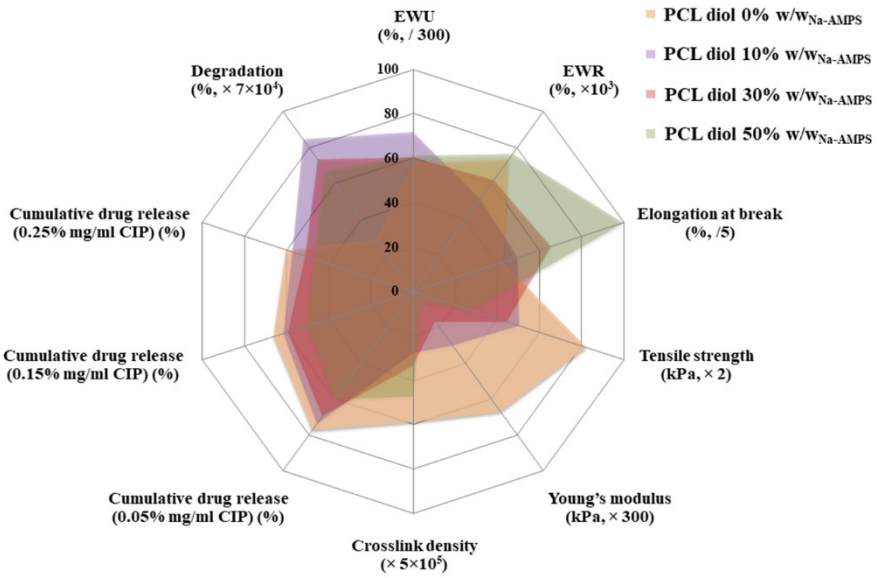

Fig. 18. The summary of properties relationships in function of hydrogel composition (with constant PEGDA crosslinker 0.75 %w/$w_{Na\text{-}AMPS}$).

Conflict of interest

The authors declare that they have no known competing financial interests or personal relationships that could have appeared to influence the work reported in this paper.

Acknowledgements

This research project was supported by Fundamental Fund 2022, Chiang Mai University and has received partial funding from the European Union's Horizon 2020 research and innovation programme under the Marie Sklodowska-Curie grant agreement No 871650 (MEDIPOL). The authors would also like to thank Chiang Mai University and the Science Achievement Scholarship of Thailand (SAST).

Data availability

The raw/processed data required to reproduce these findings cannot be shared at this time as the data also forms part of an ongoing study.

References

[1] A. Singh, P.K. Sharma, V.K. Garg, G. Garg, Hydrogels: A review, Int. J. Pharm. Sci. Rev. Res. 4 (2010) 97–105.

[2] S.K. Ghosh, A. Das, A. Basu, A. Halder, S. Das, S. Basu, M.F. Abdullah, A. Mukherjee, S. Kundu, Semi-interpenetrating hydrogels from carboxymethyl guar gum and gelatin for ciprofloxacin sustained release, Int. J. Biol. Macromol. 120 (2018) 1823–1833. https://doi.org/10.1016/j.ijbiomac.2018.09.212.

[3] A. Olad, M. Pourkhiyabi, H. Gharekhani, F. Doustdar, Semi-IPN superabsorbent nanocomposite based on sodium alginate and montmorillonite: Reaction parameters and swelling characteristics, Carbohydr. Polym. 190 (2018) 295–306. https://doi.org/10.1016/j.carbpol.2018.02.088.

[4] E.S. Dragan, Design and applications of interpenetrating polymer network hydrogels. A review, Chem. Eng. J. 243 (2014) 572–590. https://doi.org/10.1016/j.cej.2014.01.065.

[5] F. Wahid, X.H. Hu, L.Q. Chu, S.R. Jia, Y.Y. Xie, C. Zhong, Development of bacterial

cellulose/chitosan based semi-interpenetrating hydrogels with improved mechanical and antibacterial properties, Int. J. Biol. Macromol. 122 (2019) 380–387. https://doi.org/10.1016/j.ijbiomac.2018.10.105.

[6] S.A. Khan, W. Azam, A. Ashames, K.M. Fahelelbom, K. Ullah, A. Mannan, G. Murtaza, β-Cyclodextrin-based (IA-co-AMPS) Semi-IPNs as smart biomaterials for oral delivery of hydrophilic drugs: Synthesis, characterization, in-Vitro and in-Vivo evaluation, J. Drug Deliv. Sci. Technol. 60 (2020) 101970. https://doi.org/10.1016/j.jddst.2020.101970.

[7] J. Chen, M. Liu, S. Chen, Synthesis and characterization of thermo- and pH-sensitive kappa-carrageenan-g-poly(methacrylic acid)/poly(N,N-diethylacrylamide) semi-IPN hydrogel, Mater. Chem. Phys. 115 (2009) 339–346. https://doi.org/10.1016/j.matchemphys.2008.12.026.

[8] X. Hu, L. Feng, W. Wei, A. Xie, S. Wang, J. Zhang, W. Dong, Synthesis and characterization of a novel semi-IPN hydrogel based on Salecan and poly(N,N-dimethylacrylamide-co-2-hydroxyethyl methacrylate), Carbohydr. Polym. 105 (2014) 135–144. https://doi.org/10.1016/j.carbpol.2014.01.051.

[9] S. Zenoozi, G.M. Mohamad Sadeghi, M. Rafiee, Synthesis and characterization of biocompatible semi-interpenetrating polymer networks based on polyurethane and cross-linked poly (acrylic acid), Eur. Polym. J. 140 (2020) 109974. https://doi.org/10.1016/j.eurpolymj.2020.109974.

[10] S. Pourbashir, M. Shahrousvand, M. Ghaffari, Preparation and characterization of semi-IPNs of polycaprolactone/poly (acrylic acid)/cellulosic nanowhisker as artificial articular cartilage, Int. J. Biol. Macromol. 142 (2020) 298–310. https://doi.org/10.1016/j.ijbiomac.2019.09.101.

[11] N.M. Ranjha, J. Mudassir, S. Majeed, Synthesis and characterization of polycaprolactone/acrylic acid (PCL/AA) hydrogel for controlled drug delivery, Bull. Mater. Sci. 34 (2011) 1537–1547. https://doi.org/10.1007/s12034-011-0356-1.

[12] E. Su, O. Okay, Hybrid cross-linked poly(2-acrylamido-2-methyl-1-propanesulfonic acid) hydrogels with tunable viscoelastic, mechanical and self-healing properties, React. Funct. Polym. 123 (2018) 70–79. https://doi.org/10.1016/j.reactfunctpolym.2017.12.009.

[13] X. Yuan, R. Amarnath Praphakar, M.A. Munusamy, A.A. Alarfaj, S. Suresh Kumar, M. Rajan, Mucoadhesive guargum hydrogel inter-connected chitosan-g-polycaprolactone micelles for rifampicin delivery, Carbohydr. Polym. 206 (2019) 1–10. https://doi.org/10.1016/j.carbpol.2018.10.098.

[14] D.H. Hanna, G.R. Saad, Encapsulation of ciprofloxacin within modified xanthan gum-chitosan based hydrogel for drug delivery, Bioorg. Chem. 84 (2019) 115–124. https://doi.org/10.1016/j.bioorg.2018.11.036.

[15] K. Prusty, A. Biswal, S.B. Biswal, S.K. Swain, Synthesis of soy protein/polyacrylamide nanocomposite hydrogels for delivery of ciprofloxacin drug, Mater. Chem. Phys. 234 (2019) 378–389. https://doi.org/10.1016/j.matchemphys.2019.05.038.

[16] S. Basu, H.S. Samanta, J. Ganguly, Green synthesis and swelling behavior of Ag-nanocomposite semi-IPN hydrogels and their drug delivery using Dolichos biflorus Linn, Soft Mater. 16 (2018) 7–19. https://doi.org/10.1080/1539445X.2017.1368559.

[17] P.B. Kajjari, L.S. Manjeshwar, T.M. Aminabhavi, Novel interpenetrating polymer network hydrogel microspheres of chitosan and poly(acrylamide)- grafted -guar gum for controlled release of ciprofloxacin, Ind. Eng. Chem. Res. 50 (2011) 13280–13287. https://doi.org/10.1021/ie2012856.

[18] A. Alshhab, E. Yilmaz, Sodium alginate/poly(4-vinylpyridine) polyelectrolyte multilayer films: Preparation, characterization and ciprofloxacin HCl release, Int. J. Biol. Macromol. 147 (2020) 809–820. https://doi.org/10.1016/j.ijbiomac.2019.10.058.

[19] M.C. García, J.C. Cuggino, C.I. Rosset, P.L. Páez, M.C. Strumia, R.H. Manzo, F.L. Alovero, C.I. Alvarez Igarzabal, A.F. Jimenez-Kairuz, A novel gel based on an ionic complex from a dendronized polymer and ciprofloxacin: Evaluation of its use for controlled topical drug release, Mater. Sci. Eng. C. 69 (2016) 236–246. https://doi.org/10.1016/j.msec.2016.06.071.

[20] C.M. Lerche, P.A. Philipsen, H.C. Wulf, UVR: sun, lamps, pigmentation and Vitamin D, Photochem. Photobiol. Sci. 16 (2017) 291–301. https://doi.org/10.1039/c6pp00277c.

[21] W.T. Han, T. Jang, S. Chen, L.S.H. Chong, H. Do Jung, J. Song, Improved cell

viability for large-scale biofabrication with photo-crosslinkable hydrogel systems through a dual-photoinitiator approach, Biomater. Sci. 8 (2020) 450–461. https://doi.org/10.1039/c9bm01347d.

[22] X. Hu, Y. Wang, L. Zhang, M. Xu, W. Dong, J. Zhang, Fabrication of Salecan/poly(AMPS-co-HMAA) semi-IPN hydrogels for cell adhesion, Carbohydr. Polym. 174 (2017) 171–181. https://doi.org/10.1016/j.carbpol.2017.06.067.

[23] D.S. Jones, G.P. Andrews, D.L. Caldwell, C. Lorimer, S.P. Gorman, C.P. McCoy, Novel semi-interpenetrating hydrogel networks with enhanced mechanical properties and thermoresponsive engineered drug delivery, designed as bioactive endotracheal tube biomaterials, Eur. J. Pharm. Biopharm. 82 (2012) 563–571. https://doi.org/10.1016/j.ejpb.2012.07.019.

[24] Q. Yu, Y. Song, X. Shi, C. Xu, Y. Bin, Preparation and properties of chitosan derivative/poly(vinyl alcohol) blend film crosslinked with glutaraldehyde, Carbohydr. Polym. 84 (2011) 465–470. https://doi.org/10.1016/j.carbpol.2010.12.006.

[25] W. Tanan, J. Panichpakdee, S. Saengsuwan, Novel biodegradable hydrogel based on natural polymers: Synthesis, characterization, swelling/reswelling and biodegradability, Elsevier Ltd, 2019. https://doi.org/10.1016/j.eurpolymj.2018.10.033.

[26] M. Hajikhani, M.M. Khanghahi, M. Shahrousvand, J. Mohammadi-Rovshandeh, A. Babaei, S.M.H. Khademi, Intelligent superabsorbents based on a xanthan gum/poly (acrylic acid) semi-interpenetrating polymer network for application in drug delivery systems, Int. J. Biol. Macromol. 139 (2019) 509–520. https://doi.org/10.1016/j.ijbiomac.2019.07.221.

[27] R.S.H. Wong, M. Ashton, K. Dodou, Effect of crosslinking agent concentration on the properties of unmedicated hydrogels, Pharmaceutics. 7 (2015) 305–319. https://doi.org/10.3390/pharmaceutics7030305.

[28] H. Danafar, Study of the composition of polycaprolactone/poly (ethylene glycol)/polycaprolactone copolymer and drug-to-polymer ratio on drug loading efficiency of curcumin to nanoparticles, Jundishapur J. Nat. Pharm. Prod. 12 (2017) 1–9. https://doi.org/10.5812/jjnpp.34179.

[29] M.A. Bag, L.M. Valenzuela, Impact of the hydration states of polymers on their

hemocompatibility for medical applications: A review, Int. J. Mol. Sci. 18 (2017). https://doi.org/10.3390/ijms18081422.

[30] M. Tanaka, T. Hayashi, S. Morita, The roles of water molecules at the biointerface of medical polymers, Polym. J. 45 (2013) 701–710. https://doi.org/10.1038/pj.2012.229.

[31] N. Watanabe, K. Suga, H. Umakoshi, Functional hydration behavior: Interrelation between hydration and molecular properties at lipid membrane interfaces, J. Chem. 2019 (2019). https://doi.org/10.1155/2019/4867327.

[32] M.M. Fares, E. Shirzaei Sani, R. Portillo Lara, R.B. Oliveira, A. Khademhosseini, N. Annabi, Interpenetrating network gelatin methacryloyl (GelMA) and pectin-g-PCL hydrogels with tunable properties for tissue engineering, Biomater. Sci. 6 (2018) 2938–2950. https://doi.org/10.1039/c8bm00474a.

[33] Y. Qian, Z. Zhang, L. Zheng, R. Song, Y. Zhao, Fabrication and characterization of electrospun polycaprolactone blended with chitosan-gelatin complex nanofibrous mats, J. Nanomater. 2014 (2014). https://doi.org/10.1155/2014/964621.

[34] B. Guo, A. Finne-Wistrand, A.C. Albertsson, Facile synthesis of degradable and electrically conductive polysaccharide hydrogels, Biomacromolecules. 12 (2011) 2601–2609. https://doi.org/10.1021/bm200389t.

[35] C. Ji, A. Khademhosseini, F. Dehghani, Enhancing cell penetration and proliferation in chitosan hydrogels for tissue engineering applications, Biomaterials. 32 (2011) 9719–9729. https://doi.org/10.1016/j.biomaterials.2011.09.003.

[36] J.Y. Lai, Y.T. Li, Functional assessment of cross-linked porous gelatin hydrogels for bioengineered cell sheet carriers, Biomacromolecules. 11 (2010) 1387–1397. https://doi.org/10.1021/bm100213f.

[37] S.L. Edwards, J.S. Church, D.L.J. Alexander, S.J. Russell, E. Ingham, J.A.M. Ramshaw, J.A. Werkmeister, Modeling tissue growth within nonwoven scaffolds pores, Tissue Eng. - Part C Methods. 17 (2011) 123–130. https://doi.org/10.1089/ten.tec.2010.0182.

[38] M. Li, Z. Wu, C. Zhang, S. Lu, H. Yan, D. Huang, H. Ye, Study on porous silk fibroin materials. II. Preparation and characteristics of spongy porous silk fibroin materials, J. Appl. Polym. Sci. 79 (2001) 2192–2199. https://doi.org/10.1002/1097-

4628(20010321)79:12<2192::AID-APP1027>3.0.CO;2-0.

[39] N.A. Peppas, H.J. Moynihan, L.M. Lucht, The structure of highly crosslinked poly(2-hydroxyethyl methacrylate) hydrogels, J. Biomed. Mater. Res. 19 (1985) 397–411. https://doi.org/10.1002/jbm.820190405.

[40] S. Panpinit, S. amnart Pongsomboon, T. Keawin, S. Saengsuwan, Development of multicomponent interpenetrating polymer network (IPN) hydrogel films based on 2-hydroxyethyl methacrylate (HEMA), acrylamide (AM), polyvinyl alcohol (PVA) and chitosan (CS) with enhanced mechanical strengths, water swelling and antibacteria, React. Funct. Polym. 156 (2020) 104739. https://doi.org/10.1016/j.reactfunctpolym.2020.104739.

[41] S.M.H. Bukhari, S. Khan, M. Rehanullah, N.M. Ranjha, Synthesis and Characterization of Chemically Cross-Linked Acrylic Acid/Gelatin Hydrogels: Effect of pH and Composition on Swelling and Drug Release, Int. J. Polym. Sci. 2015 (2015) 1–15. https://doi.org/10.1155/2015/187961.

[42] V. Cannella, R. Altomare, G. Chiaramonte, S. Di Bella, F. Mira, L. Russotto, P. Pisano, A. Guercio, Cytotoxicity Evaluation of Endodontic Pins on L929 Cell Line, Biomed Res. Int. 2019 (2019). https://doi.org/10.1155/2019/3469525.

[43] S. Das, U. Subuddhi, Controlled delivery of ibuprofen from poly(vinyl alcohol)−poly(ethylene glycol) interpenetrating polymeric network hydrogels, J. Pharm. Anal. 9 (2019) 108–116. https://doi.org/10.1016/j.jpha.2018.11.007.

[44] A. Kapanya, R. Somsunan, R. Molloy, S. Jiranusornkul, W. Leewattanapasuk, L. Jongpaiboonkit, Y. Kong, Synthesis of polymeric hydrogels incorporating chlorhexidine gluconate as antibacterial wound dressings, J. Biomater. Sci. Polym. Ed. 31 (2020) 895–909. https://doi.org/10.1080/09205063.2020.1725862.

[45] X. Qi, W. Wei, J. Li, T. Su, X. Pan, G. Zuo, J. Zhang, W. Dong, Design of Salecan-containing semi-IPN hydrogel for amoxicillin delivery, Mater. Sci. Eng. C. 75 (2017) 487–494. https://doi.org/10.1016/j.msec.2017.02.089.

[46] X. Qi, W. Wei, J. Li, G. Zuo, X. Hu, J. Zhang, W. Dong, Development of novel hydrogels based on Salecan and poly(N-isopropylacrylamide-co-methacrylic acid) for controlled doxorubicin release, RSC Adv. 6 (2016) 69869–69881.

https://doi.org/10.1039/c6ra10716h.

[47] X. Qi, Y. Yuan, J. Zhang, J.W.M. Bulte, W. Dong, Oral Administration of Salecan-Based Hydrogels for Controlled Insulin Delivery, J. Agric. Food Chem. 66 (2018) 10479–10489. https://doi.org/10.1021/acs.jafc.8b02879.

[48] A.I. Rezk, F.O. Obiweluozor, G. Choukrani, C.H. Park, C.S. Kim, Drug release and kinetic models of anticancer drug (BTZ) from a pH-responsive alginate polydopamine hydrogel: Towards cancer chemotherapy, Int. J. Biol. Macromol. 141 (2019) 388–400. https://doi.org/10.1016/j.ijbiomac.2019.09.013.

[49] J. Sievers, K. Sperlich, T. Stahnke, C. Kreiner, T. Eickner, H. Martin, R.F. Guthoff, M. Schünemann, S. Bohn, O. Stachs, Determination of hydrogel swelling factors by two established and a novel non-contact continuous method, J. Appl. Polym. Sci. 138 (2021) 1–9. https://doi.org/10.1002/app.50326.

[50] P. Ghasemiyeh, S. Mohammadi-Samani, Hydrogels as Drug Delivery Systems; Pros and Cons, Trends Pharm. Sci. 5 (2019) 7–24. https://doi.org/10.30476/TIPS.2019.81604.1002.

[51] N.N. Li, C.P. Fu, L.M. Zhang, Using casein and oxidized hyaluronic acid to form biocompatible composite hydrogels for controlled drug release, Mater. Sci. Eng. C. 36 (2014) 287–293. https://doi.org/10.1016/j.msec.2013.12.025.

[52] A. Rezaei, A. Nasirpour, Evaluation of Release Kinetics and Mechanisms of Curcumin and Curcumin-β-Cyclodextrin Inclusion Complex Incorporated in Electrospun Almond Gum/PVA Nanofibers in Simulated Saliva and Simulated Gastrointestinal Conditions, Bionanoscience. 9 (2019) 438–445. https://doi.org/10.1007/s12668-019-00620-4.

[53] P. Ilgin, H. Ozay, O. Ozay, A new dual stimuli responsive hydrogel: Modeling approaches for the prediction of drug loading and release profile, Eur. Polym. J. 113 (2019) 244–253. https://doi.org/10.1016/j.eurpolymj.2019.02.003.

[54] S. Dash, P.N. Murthy, L. Nath, P. Chowdhury, Kinetic modeling on drug release from controlled drug delivery systems, Acta Pol. Pharm. - Drug Res. 67 (2010) 217–223.

[55] J. Li, D.J. Mooney, Designing hydrogels for controlled drug delivery, Nat. Rev. Mater. 1 (2016) 1–18. https://doi.org/10.1038/natrevmats.2016.71.